

# Sphingolipids in Ventilator-Induced Lung Injury

BY

VIDYANI SURYADEVARA

B.Tech., Osmania University, India, 2013

THESIS

Submitted as partial fulfillment of the requirements  
for the degree of Master of Science in Bioengineering  
in the Graduate College of the  
University of Illinois at Chicago, 2014

Chicago, Illinois

Defense Committee:

Dr. Viswanathan Natarajan, Chair and Advisor, Department of Pharmacology

Dr. Thomas Royston

Dr. Jeffrey R. Jacobson, Medicine, Pulmonary, Critical Care, Sleep & Allergy

This thesis is dedicated to my parents and to my mentor, Dr. Viswanathan Natarajan.

## ACKNOWLEDGEMENTS

It is my great pleasure to thank the many people who have contributed.

I would like to extend my heart-felt gratitude to Dr. Viswanathan Natarajan for his meticulous training and mentorship. I am ever grateful to him for his great deal of time and effort in shaping my project and for the opportunity to make me a part of his intellectual environment and his encouragement and guidance throughout my graduate studies and research. His patience and enthusiasm in research had motivated me to work harder in achieving perfection. In addition, he was always accessible and willing to help me with my research and during any exigency.

In addition to my advisor Dr. Natarajan, I would like to thank the rest of my committee members, Dr. Thomas Royston and Dr. Jeffrey Jacobson, for their time in reviewing this thesis and for their thoughtful advice and feedback.

I would like to thank Dr. Peter Usatyuk for training me with immunofluorescence and timely advice and invaluable assistance. I wish to thank Dr. Panfeng Fu for his expertise in animal work and providing me training. I would like to thank Dr. Longshuang Huang for his extremely constructive and detailed suggestions. I gratefully acknowledge Dr. Anantha Harijith and Dr. Fernando Testai for their patience and answers to my continuous stream of questions, giving a solid technical foundation for my thesis.

I would like to extend my gratitude to Dr. Evgeny Berdyshev for the LC-MS/MS measurements, Dr. Balaji Ganesh, Director, Flow Cytometry Core and the Research Histology Laboratory (Department of Pathology, UIC). I also thank Dr. Sekhar P Reddy and his research

team for availing me the opportunity to utilize their resources for my experiments which have composed an integral part of my project.

My special acknowledgements to David Ebenezer for training me on western blots and also his valuable insights and ever-encouraging words. I also thank Mark Shaaya, Justin Sysol, Eleftheria Letsiou and Indira Elangovan, the pursuit of my Masters wouldn't have been such a fruitful and fun-filled journey without them. On a personal note, I would like to thank Mrs. Lakshmi Natarajan for her incredulous love and support, making my time at UIC memorable. I have benefitted greatly from their insights of my temporary advisor, Dr. G. Ali Mansoori. I would also like to thank all my lab members and members of the Pulmonary Division who have helped me in one way or another through this wonderful journey.

Most importantly, I would like to thank my parents, brother, family and undergraduate mentors for their never-ending support. They have instilled confidence in me and taught by example the meaning of hard work. Thanks to my roommates and friends for being a constant source of inspiration at all times. Without their support and faith in my success, I would never have made it so far.

## TABLE OF CONTENTS

Chapter	Page Number
<b>I. INTRODUCTION.....</b>	<b>01</b>
1. Forces in the lung.....	01
2. Mechanical ventilation.....	03
2.1 Historical Perspective.....	03
2.2 Physics behind mechanical ventilation.....	06
3. Cyclic stretch.....	08
4. Sphingolipids.....	11
4.1 Biosynthesis and catabolism of sphingolipids. ....	13
4.2 Role of sphingolipids in Apoptosis.....	16
4.3 Role of sphingolipids in membrane integrity.....	17
5. The Flexcell® FX- 5000™ Tension System.....	17
i. Loading posts.....	18
ii. Flexible-bottomed Bioflex plates.....	20
iii. Flexcell® Tension system.....	20
<b>II. EXPERIMENTAL PROCEDURES.....</b>	<b>22</b>
<b>INVIVO</b>	
1.Generation of wild type and heterozygous/ homozygous mice.....	22
2.Mechanical ventilation.....	23
3.BAL Collection and quantitative measures of VILI.....	24
4. Lung Tissue harvesting and analysis. ....	25

a. Electrospray ionization liquid chromatography tandem mass spectrometry. ....	25
b. Western blotting.....	27
c. RNA isolation and RT-PCR.....	28
d. Lung histology.....	29
e. TUNEL staining. ....	29
INVITRO.....	29
5.Cyclic stretch.....	30
a. Lipid Extraction and Sample Preparation for LC/MS/MS for analysis of Sphingoid bases .....	30
b. Western blotting.....	31
c. RNA isolation and RT-PCR.....	32
6.Immunofluorescence.....	33
7.Flow cytometry analysis for Apoptosis. ....	33

### III. RESULTS

#### *IN VIVO*

1. Expression of sphingoid bases and sphingolipids metabolizing enzymes after VILI.	
i. Levels of sphingoid bases in mouse lung and BALF after VILI.....	35
ii. Expression of sphingolipid metabolizing enzymes in mouse lung after VILI.....	36
iii. Expression of S1P Lyase in BALF after VILI.....	37
2. Role of sphingolipid metabolizing enzymes in VILI.....	38
i. Assessment of VILI in 129SV wild type and <i>Sgpl1</i> <sup>+/-</sup> mice.....	39
ii. Alveolar infiltration in wild type and <i>Sgpl1</i> <sup>+/-</sup> mice after VILI.....	41

iii.	TUNEL positive cells after VILI in 129SV wild type and <i>Sgpl1</i> <sup>+/-</sup> mice....	42
iv.	Assessment of VILI in C57Bl6 WT and <i>Sphk1</i> <sup>-/-</sup> mice.....	44
v.	Alveolar infiltration after VILI in C57Bl6 wild type and <i>Sphk1</i> <sup>-/-</sup> mice.....	45

**IN VITRO**

3.	Expression of sphingoid bases and sphingolipids metabolizing enzymes in MLE-12 to cyclic stretch. ....	47
i.	Expression of S1P Lyase in epithelial and endothelial cells after cyclic stretch.....	47
ii.	Expression levels of sphingoid bases, S1P Lyase in MLE-12 cells after physiological and pathophysiological conditions of cyclic stretch.....	47
4.	Effects of CS on cell apoptosis.....	48
i.	Biochemical Markers of apoptosis.....	48
ii.	Flow cytometry for analysis of apoptosis.....	49
5.	Cell reorientation after cyclic stretch.....	51
6.	Effect of inhibition of S1P Lyase by 4-DP.....	51
i.	Effect of 4-DP on cyclic stretch induced apoptosis.....	51
ii.	Effect of 4-DP on paracellular gaps caused by high magnitude stretch....	52
<b>IV.</b>	<b>DISCUSSION.....</b>	<b>54</b>
<b>V.</b>	<b>CITED LITERATURE .....</b>	<b>57</b>
<b>VI.</b>	<b>APPENDIX.....</b>	<b>62</b>
<b>VII.</b>	<b>VITA.....</b>	<b>65</b>

## LIST OF FIGURES

Figure	Page Number
1. Surface tension acting in the alveoli.....	2
2. Iron lungs using for polio treatment at Hynes Memorial Hospital in Boston. USA, 1955.....	4
3. Different modes of mechanical ventilation.....	5
4. Salient features of VILI.....	8
5. Illustration of the cyclic opening and closure of alveoli during mechanical ventilation at 0 PEEP .....	9
6. The topology of sphingolipid metabolites and enzymes in the cell.....	14
7. Sphingolipid metabolism.....	15
8. Sphingolipid rheostat affecting survival and function.....	16
9. BioFlex® baseplate showing the Loading Stations™ with six loading posts (P) and BioFlex® culture plates in red, rubber gaskets.....	18
10. Equibiaxial strain application to cells plated on a StageFlexer® Membrane and clamped in a StageFlexer® Strain Device.....	19
11. Waveform plot showing typical sinusoidal waveform.....	21
12. Schema showing the analysis of VILI.....	24
13. Levels of sphingoid bases in mouse lung after VILI.....	35
14. Levels of sphingoid bases in BALF after VILI.....	36
15. Expression of S1P Lyase, SphK1, SphK2 and actin in mouse lung after VILI.....	36
16. mRNA levels of S1PLyase and SphK1, SphK2 in mouse lung after VILI. ....	37

17. Expression of sphingolipid metabolizing enzymes in BALF after VILI.....	37
18. Genotyping for <i>Sgpl1</i> <sup>+/+</sup> and <i>Sgpl1</i> <sup>+/-</sup> mice.....	38
19. S1P, mRNA levels of wild type and <i>Sgpl1</i> <sup>+/-</sup> mice.....	39
20. Assessment of VILI in WT and <i>Sgpl1</i> <sup>+/-</sup> mice.....	39-41
21. Alveolar infiltration after VILI in wild type and <i>Sgpl1</i> <sup>+/-</sup> mice.....	42
22. TUNEL positive cells after VILI in wild type and <i>Sgpl1</i> <sup>+/-</sup> mice.....	43
23. Assessment of VILI in WT and <i>Sphk1</i> <sup>-/-</sup> mice.....	44, 45
24. Alveolar infiltration after VILI in wild type and <i>Sphk1</i> <sup>-/-</sup> mice.....	46
25. S1P Lyase in expression after cyclic stretch.....	47
26. Expression levels of sphingoid bases, S1P Lyase in MLE-12 cells after cyclic stretch.....	48
27. Cleavage of apoptotic proteins Caspase-3 and PARP.....	49
28. MLE-12 cells incubated with Annexin V and PI .....	50
29. Late apoptotic and early apoptotic cells after different magnitudes of cyclic stretch.....	50
30. Actin remodeling and gap formation after cyclic stretch .....	51
31. Effect of S1P Lyase inhibition on apoptosis.....	52
32. Effect of S1P Lyase inhibition on paracellular gap formation.....	53

## ABBREVIATIONS

BALF	Bronchoalveolarlavage fluid
CS	Cyclic stretch.
HLMVEC	Human Lung microvascular endothelial cells
MLE-12	Mouse transformed lung epithelial cells
S1P	Sphingosine-1-phosphate
S1PL	Sphingosine-1-phosphate Lyase
SA	Surface Area
SphK1	Sphingosine Kinase1
SphK2	Sphingosine Kinase 2
TLC	Total Lung Capacity
VILI	Ventilator induced lung injury

## SUMMARY

Mechanical forces acting in various organs in the body affect the homeostasis and normal functioning. Lung is one of the most dynamic organs in the human body that is subjected to various physical and mechanical cues inferred from blood flow, breathing and surface tension; right from developmental stages and throughout life. Mechanical deformation of the lung tissue due to various forces acting on different regions of the lung, leads to over distention of the lung, resulting in a series of mechanosensing and mechanotransduction events at the cellular and organ level. This study aims to investigate the effect of mechanical stress on sphingolipid metabolism in the lungs, particularly in the alveolar epithelium, with the goal to better understand the molecular mechanisms that occur during ventilator - induced lung injury (VILI) and to identify new targets for therapy. Sphingolipids have been implicated in various lung pathologies. However, little is known about the role of sphingolipids in VILI. A rodent model of ventilator induced lung injury and *in vitro* model of alveolar epithelial cells subjected to pathophysiological mechanical stress were used.

Mechanical ventilation at high tidal volume (30 ml/kg, 4 hrs) in mice enhanced S1P lyase (S1PL) expression, elevated ceramide levels, decreased sphingosine-1-phosphate (S1P) levels in lung tissue, thereby leading to cytoskeletal rearrangement, lung inflammation and injury and apoptosis. Accumulation of S1P in cells is a balance between its synthesis catalyzed by sphingosine kinase (SphK) 1 and 2 and catabolism mediated by S1P phosphatases and S1PL. Thus, the role of S1P Lyase and SphK1 in VILI was investigated by studies using S1PL<sup>+/-</sup> and SphK1<sup>-/-</sup> mice. Partial genetic deletion of S1P L (*Sgpl1*<sup>+/-</sup>) partly protected VILI in mice. On the other hand, the genetic deletion of SphK1 enhanced VILI in mice. Simulating VILI in the laboratory requires stretching of lung alveolar tissue. *In vitro* cyclic stretch of the cells mimics the constant collapse and reopening of the alveoli during mechanical ventilation. Mechanical cyclic stretch of

human lung microvascular endothelial cells (HLMVEC) and murine alveolar type II epithelial (MLE12) cells increased S1P Lyase protein expression. Also, the pathophysiological levels of cyclic stretch i.e. 18% stretch stimulated epithelial cell apoptosis, disrupting barrier function and differential expression of various sphingoid bases, when compared to physiological relevant magnitude of stretch i.e. 5% cyclic stretch. Pre-treatment of alveolar epithelial cells with S1PL inhibitor 4-DP effectively promoted cell barrier recovery and minimized cell apoptosis caused by 18% cyclic stretch, suggesting the regulatory roles of S1P in VILI. The *in vivo* and *in vitro* results identify a novel role for intracellularly generated S1P in protection against VILI and suggest S1PL as a potential therapeutic target.

## **1. INTRODUCTION**

In biological systems, mechanical forces are as important as chemicals and genes. The external forces like tension, compression, and shear acting in the body result in deformation of the tissues like lungs, arteries, muscle, bladder, tendons etc. Physical cues from the environment play a vital role in the body development and function of the organ and regulate cell and tissue behavior. Tissue geometry has an effective architecture for each function, which adapts to its surroundings. The mechanical forces in the body include shear stresses in blood vessels, blood pressure, gravity on bone and cartilage, stretch of skin and muscles during movements of arms and many more.

The mechanical forces also regulate tissue differentiation and determine their fate during development [1]. They play a vital role right from fertilization of egg, divisions of cells in early embryo to formation of first tissue and organs, morphogenesis of tissues and organs, and also in modulating the maintenance of tissue architecture. They also govern the functional process at many forces and mechanotransduction leading to disease. Physical compaction in some tissues induces transcriptional factors for organ regeneration.

At the cellular level, the cells pull on their adhesions on other cells and onto the extracellular matrix (ECM) on which they adhere. They're their anchoring scaffold. The ECM orients the cells and provides a scaffold for their renewal and repair. The extracellular mechanical signals are mechanotransduced into intracellular biochemical changes and gene expression levels [2].

### **1. Forces in the Lung:**

Lung is a dynamic organ, subjected to various forces right from it's development in early stages, growth, metabolism and normal function. These forces have a vital role during the physiological as well as the pathophysiological conditions of the lung. Lung is routinely exposed to biophysical forces in the forms of:

- i. Shear stress (SS) on the endothelial cells due to blood flow;
- ii. Mechanical strain levied by the respiratory cycles on the epithelial cells lining the alveoli in the lungs and
- iii. Surface tension due to cohesive forces between the air and alveoli during gaseous exchange.

**Surface tension:** The alveolar type-II cells in the lung secrete surfactant, which helps in reducing the surface tension, thereby mechanically stabilizing the lung alveoli [3]. Applying the Laplace Law to the dynamic alveoli, which change their surface tension proportional to their size, to maintain alveolar stability, it is estimated that the surface tension should be reduced proportional to the reduction in the size of the alveoli. Also in interconnected alveoli, the pressure is modulated accordingly such that they will have the same surface tension.

Law of Laplace: 
$$P = \frac{2\gamma}{r} \dots\dots\dots \text{Equation 2 [4]}$$

Here  $\gamma$  = surface tension,  $r$  = radius of the alveolar sac and  $P$  is the pressure in the alveoli.

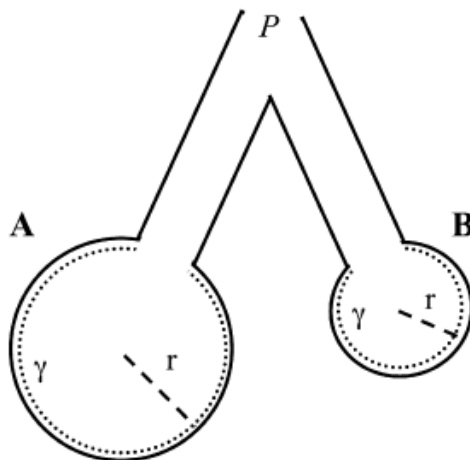


**Fig. 1: Surface tension acting in the alveoli. [4]**

In this study we, focus on the effect of mechanical ventilation in the lungs, wherein the ventilator exerts various forces on the lung.

## **2. Mechanical Ventilation:**

As inferred from [5] The American Association for Respiratory Care infers mechanical ventilation to include various invasive and non-invasive ventilator models to facilitate breathing, mainly during respiratory failure. However, the mechanical ventilation in any form cannot be used to cure any disease. It is just given to ameliorate the health of the patient.

Mechanical ventilation (MV) is done in various respiratory disorders as well other physiological conditions. MV is done to tender protection to the lung during bradypnea or apnea with respiratory arrest, tachypnea, acute respiratory distress syndrome, hypotension, obtundation or coma, neuromuscular disease, respiratory muscle fatigue, clinical deterioration, shock, trauma, sepsis, or pneumonia. It renders passable gas exchange while giving rest to the respiratory muscles. Also, elderly people with breathing difficulties are put onto mechanical ventilator.

### **2.1 Historical perspective:**

In 1929 mechanical ventilation was done using the Drinker and Shaw tank-type ventilator, this was one of the first negative-pressure machines and provided non-invasive ventilation. They were used during the polio outbreak in 1955, wherein the patient's neck was engulfed by the metal cylinder. The patient's chest was expanded due to the negative pressure being created in the chamber by the vacuum pump, whereas the termination of vacuum resulted in zero negative pressure. The repeated cycles changed the chest geometry and allowed inhalation and exhalation.



**Fig 2: Iron lungs using for polio treatment at Hynes Memorial Hospital in Boston. USA, 1955**

Later, they were replaced by positive pressure ventilators, with the first non-invasive ventilation being used in 1955, wherein the endotracheal tube was introduced into the trachea (endotracheal intubation). The positive pressure created by this insertion of the endotracheal tube in the lungs, inflated the lungs.

This initial method of ventilation was cumbersome and caused discomfort to the patients. Over the years, ventilators have advanced along with novel strategies of ventilation and in the present day, mechanical ventilation is classified into two groups:

- i. Invasive mechanical ventilation.
- ii. Non-invasive mechanical ventilation

In invasive mechanical ventilation, an endotracheal tube or tracheotomy cannula is used for mechanical ventilation, whereas in the non-invasive mechanical ventilation, nasal cannula or face

masks support the respiration. This is generally performed in COPD and pneumonia patients who can breathe and cough effectively on their own and are conscious and cooperative to the treatment.



**Negative- pressure ventilation**



**Positive-pressure ventilation**



**Invasive mechanical ventilation**



**Non-invasive mechanical ventilation**

***Fig.3 Different modes of mechanical ventilation***

Non-invasive ventilation during exercise has shown to be very effective to attenuate the inspiratory muscle effort and has shown consistent ameliorated exercise outcomes in COPD patients [6]. On the other hand, in patients ventilated by tracheostomy or an endotracheal tube, bacterial infections in the lung lead to nosocomial pneumonia called ventilator associated pneumonia, thereby increasing the mortality rates [7].

In the case of hypercapnic forms of acute respiratory failure characterized by dyspnea and encephalopathy, mechanical ventilation was observed to reverse the clinical abnormalities [8]. Improved tolerance towards fiber optic bronchoscopy and less side-effects was made possible by simultaneous non-invasive mechanical ventilation [9].

Potential lung donors are subjected to mechanical ventilation to prevent lung injury, as the donors run the risk of neurogenic pulmonary edema, during brain death [10]. In infants with respiratory failure, non-invasive respiratory support has shown to be more appropriate than mechanical ventilation or intubation [11]. Though mechanical ventilation (MV) is being used for the treatment of disease, it has several limitations, sometimes worsening the disease. MV can exacerbate lung injury leading to ventilator induced lung injury when healthy patients are ventilated [12].

The deleterious effects of MV are attributed to hemodynamic compromise and some of the complications of MV include: oxygen toxicity, volutrauma, barotrauma, auto PEEP, diaphragm atrophy, ventilator associated pneumonia, bacterial infections, decreased cardiac output, collapsed lung, lung damage. Ventilation at high lung volume causes air leaks and overdistention of the lungs. Low lung volume ventilation causes lung inhomogeneity and atelectrauma [13]. This necessitates the need for optimizing lung-protective ventilator strategies.

## **2.2 Physics behind mechanical ventilation:**

The consummate ventilator strategy entails the interplay of pressure and physics of flow involved, expressed as positive pressure, respiratory rate, trigger and tidal volume. The trigger is what causes the mechanical ventilator to start a breath cycle. The trigger has to be set optimally so that patient doesn't have to put too much effort for respiration nor that it's difficult for the patient

to breathe. Positive-end-expiratory- pressure (PEEP) is the amount of air/ pressure still in the lungs at the end of exhalation. This pressure is essential to prevent alveolar collapse. The respiratory rate is the number of breaths being delivered by the ventilator per minute. It regulates the CO<sub>2</sub> levels. Tidal volume or the depth of breathing is the volume of gas inspired or expired during each respiratory cycle. The total amount of air coming into the patient's lung with each breath is given by minute ventilation.

$$\text{Minute Ventilation} = \text{Respiratory Rate} \times \text{Tidal Volume} \dots \text{Equation 1[14]}$$

Flow rate is the rate at which the set tidal volume is being delivered and it affects the time for exhalation. Flow pattern is the rate of change of flow rate. Fraction of inspired oxygen FiO<sub>2</sub> is the percentage of oxygen in the air that is being delivered to the lungs. This is to bring the patient arterial oxygen pressure up to his/her target arterial oxygen. Once this is attained, the oxygen pressure is then lowered to avoid oxygen toxicity.

In the present study, we focus on the effect of ventilation in the settings at high tidal volume and 0 PEEP and study its transduction into ventilator-induced lung injury. The salient features of ventilator induced lung injury include: trigger of inflammatory cascades, cell-cell and cell-membrane disruption, protein-rich alveolar edema and increased lung vascular permeability. The cyclic opening and closure of the airways and their collapse during ventilation results in the increase in the shear forces and stretch leading to surfactant dysfunction, activation of inflammatory responses by cytokines and lung injury.

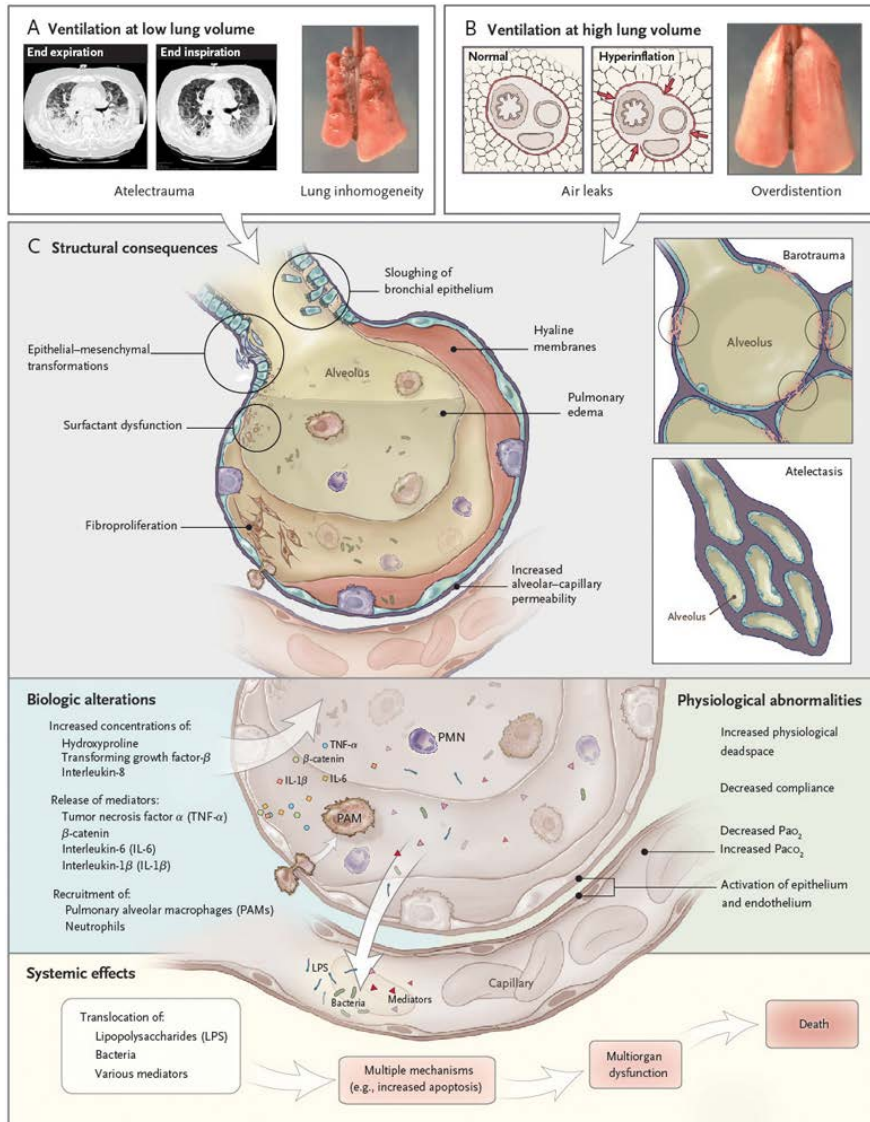


**Fig. 4: Salient features of VILI**

“Reproduced with permission from (Slutsky AS, Ranieri VM Ventilator-induced lung injury. N Engl J Med. 2013 Nov 28; 369(22):2126-36), Copyright Massachusetts Medical Society.

### 3. Cyclic stretch

During mechanical ventilation of the lungs, most cell types in the lung, mainly the alveolar epithelial cells and the capillary endothelial cells are subjected to stretch. Alveolar epithelium is denuded during acute lung injury or abnormal stress on the lungs, resulting in loss of membrane

integrity in the alveolar lining, thereby making it permeable to large molecules [15]. This loss of epithelial monolayer integrity with lung injury can be seen by the appearance of soluble fragments of E-Cadherin in the alveolar liquid lining i.e. the lavage fluid. {Thammanomai, 2013 #33}E-cadherin, expressed in the epithelial tissues in the lung has a transmembrane domain linking the epithelial cells and has a key role in cell-cell mechanotransduction.

During inflation of the lungs with high volumes, the alveolar epithelium experiences stretch due to repeated opening and closure of the airways and alveoli. This cyclic opening and closure of the alveoli can be mimicked *in vitro* by equibiaxial cyclic stretch. The adjacent endothelial cells also experience similar distension during stretch, as they are attached to the epithelial cells by means of tight junctions.

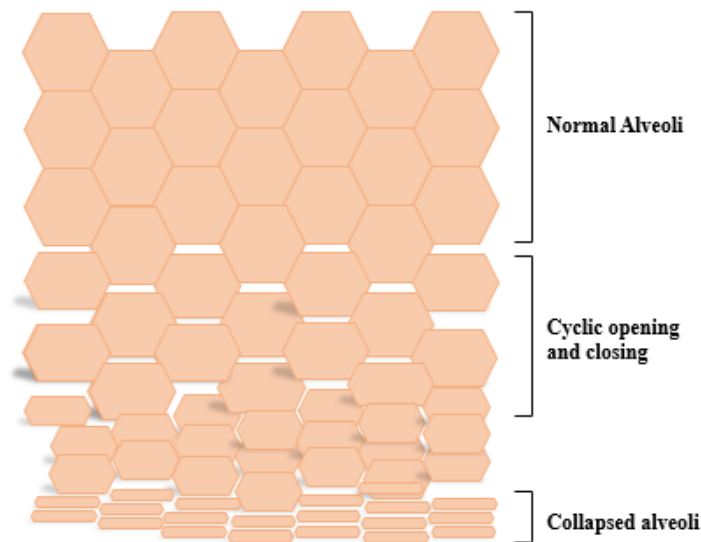


**Fig.5: Illustration of the cyclic opening and closure of alveoli during mechanical ventilation at 0 PEEP.**

Tschumperlin and Margulies [16] suggest 34–35% increase in the alveolar epithelial cell surface area if lung volume increases from 40% to 100% of total lung capacity. The epithelial layer

lining the alveolus is majorly responsible for the alveolar flooding. The epithelial basement membrane surface area (EMBSA) is modulated by the degree of force being exerted on the epithelial lining in the alveoli. The extent deformation of the EMBSA due to the lung volume was given by:

$$\% \Delta SA = 0.0057 (\% TLC)^2 - 0.2608 (\% TLC) + 4.8021 \dots \dots \dots \text{equation 3 [17]}$$

where SA = epithelial basement membrane surface area.

TLC = total lung capacity

The long-term or short-term changes that the cell undergoes during breathing is mimicked by the cyclic stretch. During cyclic stretch, the cells orient perpendicular to the direction of stretch. The stress fibers in the cell reorient perpendicular to the direction of stretch. This was proved by several mathematical models invitro [18].

The cyclic stretch imposed on the cells accords the evaluation of the cellular elongation in response to the elastomere base deformation of the culture plates [19]. The cell behavior is studied in terms of its response to the force on the underlying substrate. The cell attaches to the underlying substrate by means of focal adhesions, which are connected to the cell cytoskeleton at the other end. Hence, the deformation of the focal adhesions has an important role in the reorientation.

The orientation of the cell can be estimated by computing the circular variance  $cv$ .  $N_{FA}$

$$\text{Circular variance, } cv = 1 - \frac{1}{N_{fa}} \sqrt{(\sum_1^{N_{fa}} \sin(2\alpha))^2 + (\sum_1^{N_{fa}} \cos(2\alpha))^2}$$

.....Eq.5 [20]

, where  $N_{FA}$  = number of focal adhesions,

$\alpha$  = angular distribution of focal adhesions.

The decreased phosphorylation of focal adhesion kinases, resulting in reduced cell adhesion and abridged migration has already been shown to induce several cellular functions including the loss of membrane integrity which would lead to acute lung injury.

Cyclic stretch of the cells would result in mechanosensing and mechanotransduction, wherein the mechanical forces are converted into several biochemical changes inside the cell, thereby initiating various signaling cascades inside the cell. The mechanotransduction is initiated at the cell membrane by means of tight junction proteins, focal adhesions, ion channels, integrins that mediate inside-out and outside in signaling and also lipids on the cellular membrane like the sphingomyelinases.

In this study, we focus on the mechanotransduction of the forces into biochemical changes in modulating one or many of the components of sphingolipid pathway.

#### **4. Sphingolipids**

Lipids constitute about 50% of the total mass of most of the animal cell membranes.  $1\mu\text{m} \times 1\mu\text{m}$  area of lipid bilayer has about  $10^9$  lipid molecules in the plasma membrane. The most abundant membrane lipids are phospholipids, which include sphingolipids like sphingomyelin and sphingosine. All sphingolipids are derived from the aliphatic amino alcohol sphingosine.

Sphingolipids, are bioactive lipids and are the major constituents of the eukaryotic cell membranes, enriched in lipid rafts, having a role in the cell architecture and also in protecting the cell from mechanical and chemical cues. The sphingolipids were named in 1884 after the Greek mythological creature, the “Sphinx” by J.L.W. Thudichum, owing to their enigmatic nature [21]. Later, the term “sphingolipide” was introduced by Herbert Carter and colleagues in 1947.

There are at least 400 head group variants of sphingolipids, out of which sphingolipids, free sphingoid bases and sphingolipid degradation products such as sphingomyelin, sphingosylphosphorylcholine, ceramide, sphingosine, and their phosphorylated forms ceramide 1-phosphate (C1P) and sphingosine 1-phosphate (S1P) are the major sphingoid bases that have a prominent role in cell signal transduction, adhesion, angiogenesis, apoptosis, cell proliferation, growth arrest, differentiation, migration, senescence, or intracellular trafficking [22, 23].

The cellular membranes like endoplasmic reticulum, golgi complex, plasma membrane, inner and outer mitochondrial membrane have a wide distribution of sphingolipids. They are abundantly generated in the endoplasmic reticulum and golgi complex and are translocated to the cell membrane by the cytoplasm. [24]

In recent years, the mystery of the many hues of the sphingolipid metabolites has been unraveled with the advent of research techniques in the field. Valuable insights into interpreting the physiological and pathophysiological role of sphingolipid metabolites are being made possible by the generation of knockout mice by the ability to clone the regulatory proteins and enzymes involved in the sphingolipid metabolism. The therapeutic potential has been unleashed by the development of inhibitors of signaling enzymes and also specific agonists and antagonists of the S1P receptors. Also, the sphingosine analogue FTY720 [25], which is already in the phase III clinical trials for the treatment of multiple sclerosis, has shown to be a novel therapeutic agent in diseases caused by abnormal sphingolipid metabolism. The concurrent analysis and quantification of sphingolipid species by positive ion electrospray ionization (ESI) liquid chromatography-tandem mass spectrometry (LC-MS/MS) has played an indispensable role in elucidating their role in disease [26].

#### **4.1 Biosynthesis and catabolism of Sphingolipids:**

The *de novo* synthesis starts at the cytoplasmic face of the endoplasmic reticulum. The enzyme serine palmitoyl transferase condenses serine and palmitoyl CoA to yield 3-ketodihydrosphingosine [27]. 3-ketodihydrosphingosine is reduced to dihydrosphingosine (sphinganine), which is then acylated by dihydroceramide synthases, producing dihydroceramide, which in turn is converted to ceramide [28]. At this juncture of the sphingolipid metabolism pathway, ceramide acts as the branch point as it is produced not only from the *de novo* pathway, but also by the breakdown of membrane sphingomyelin by sphingomyelinases [29]. In mammalian cells, five major sphingomyelinases i.e. acid sphingomyelinase, neutral sphingomyelinases 1, 2 & 3 and acidic sphingomyelinase have been cloned and characterized.

Ceramide is broken down to sphingosine by the enzyme ceramidase. The subsequent conversion of sphingosine to S1P is catalyzed by sphingosine kinase (SphK), and there are two distinct isoforms of sphingosine kinase enzyme, namely SphK1 and SphK2.

S1P is dephosphorylated to sphingosine by S1P phosphatases (S1PP) or lipid phosphate phosphatases. Intracellularly, S1P can be degraded either by reversible dephosphorylation to sphingosine by two S1P phosphatases, SPP1 and SPP2; or irreversibly cleaved at C2-C3 bond by the pyridoxal phosphate dependent enzyme sphingosine 1 phosphate lyase to yield trans-2-hexadecenal and phosphoethanolamine [31]. This is the only terminal point of the sphingolipid pathway.



On the other hand, S1P can also be released out into the extracellular environment. The extracellular S1P can bind to the S1P receptors named S1PR<sub>1</sub>–S1PR<sub>5</sub>. There are five distinct high-affinity class A G protein –coupled cell surface receptors (GPCRs). [32] These S1P receptors have vital role in various organs in the human body including brain, heart, lungs, spleen, liver, thymus, skeletal muscle, kidney, lymphoid, testis, and skin. In addition, the S1P signaling system also comprises the transporter molecules like Spinster-2 (Spns2) which allow the inside-out signaling of S1P [33].

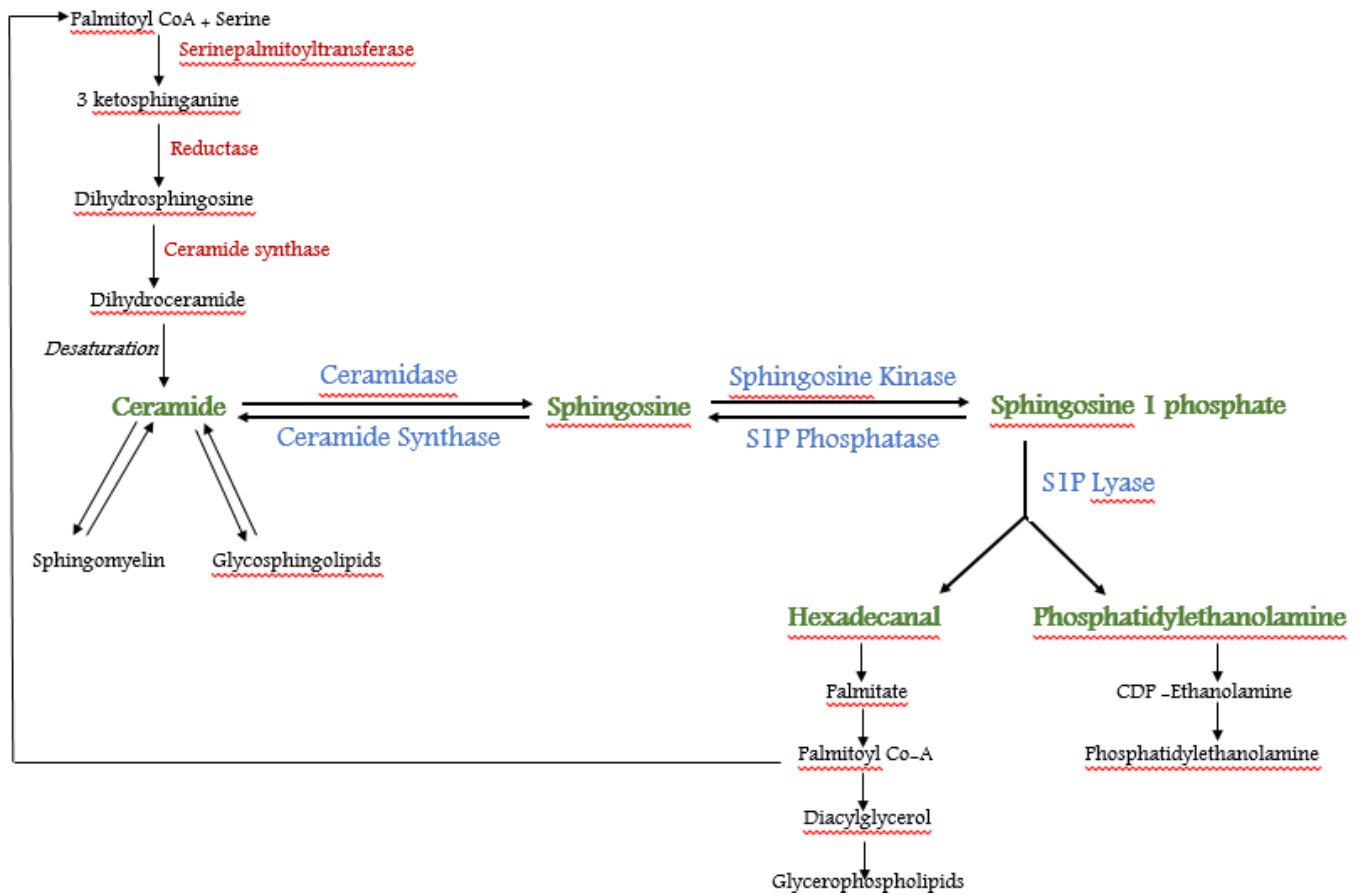


**Fig 7: Sphingolipid metabolism**

The role of disrupted sphingolipid metabolism is underscored in various animal diseases. Each of the component in the sphingolipid generation and metabolism pathway has a prominent role in the disease pathology.

#### **4.2 Role of sphingolipids in apoptosis:**

Ceramide is the vital sphingoid base that has a potential role in many signaling cascades leading to apoptosis. Mitochondrial ceramide and nuclear ceramide and action of the ceramides at the plasma membrane contribute to ceramide mediated apoptosis [34]. Sphingolipids also regulate apoptosis in lysosomes and endoplasmic reticulum of the cell. There is an intense change in the ceramide levels, even due to the minor changes in the sphingomyelinase levels. This is due to the abundance of Sphingomyelinase in higher magnitude of concentrations than ceramide.[35]. A wide range of stressful stimuli cause membrane sphingomyelin and to lesser extent other complex sphingolipids to rapidly metabolize to the bioactive sphingolipid intermediate ceramide and subsequently to sphingosine, which are pro-apoptotic.



**Fig8: Sphingolipid rheostat affecting survival and function**

### **4.3 Role of sphingolipids in membrane integrity:**

Sphingosine 1-phosphate (S1P) is a biologically active lipid that has an important role in regulating the growth, survival and migration of mammalian cells. The levels of S1P in the cell are tightly regulated in a spatial-temporal manner by the balance between its synthesis and degradation [36]. The S1P levels are tightly regulated by the components of sphingosine-1-phosphate rheostat (S1P Lyase and Sphingosine Kinases SphK1 & SphK2). S1P modulates the barrier function by having an important role in cytoskeletal rearrangement, adherens junction reassembly and also focal adhesion remodeling. In addition to be responsible for maintaining the barrier integrity, it also has a role in barrier protection during stress or injury to the cell.

## **5. The Flexcell® FX- 5000™ Tension System**

The Flexcell® FX- 5000™ Tension System is used to culture cells in a mechanically active environment to study the biochemical and physiological changes in the cells, elucidating into the pathophysiological processes. It applies either uniaxial or equibiaxial tension to monolayer of cells in culture. The cultured cells were subjected to regulated magnitude of strain at desired frequency by this Flexcell® Tension system, which comprised of Loading Stations™ specially designed for use with BioFlex®, flexible-bottomed culture plates. In the biaxial strain, the adherent cells were deflected downward using negative pressure, thereby imparting strain to the culture layer [38]. The desired % elongation of the substrate is being controlled by controlling the vacuum pressure created from the vacuum pump is controlled using the FX-5000 software.

The components of the Flexcell System include:

- iv. Loading posts

- v. Flexible-bottomed Bioflex plates
- vi. Flexcell® Tension system

i. **Loading posts:**

The BioFlex® Loading Stations™ provide uniform radial and circumferential strains to cells cultured on flexible membranes. The loading posts may be either cylindrical or arctangle. The cylindrical loading posts provide equibiaxial strain, whereas the uniaxial strain is provided by the Arctangle Loading posts:

As shown in figure 1, the loading stations comprise a 3.3” x 5” Lexan® plate and six removable Delrin® planar faced cylinders or posts. The posts are positioned on the Lexan® plate such that each is centered beneath the rubber membrane of each well of a BioFlex® culture plate. Upon application of vacuum to a BioFlex® culture plate\* with a Flexcell® Tension System, the membrane deforms across the post face creating uniform equibiaxial strain (Fig. 2). (Reference 49)

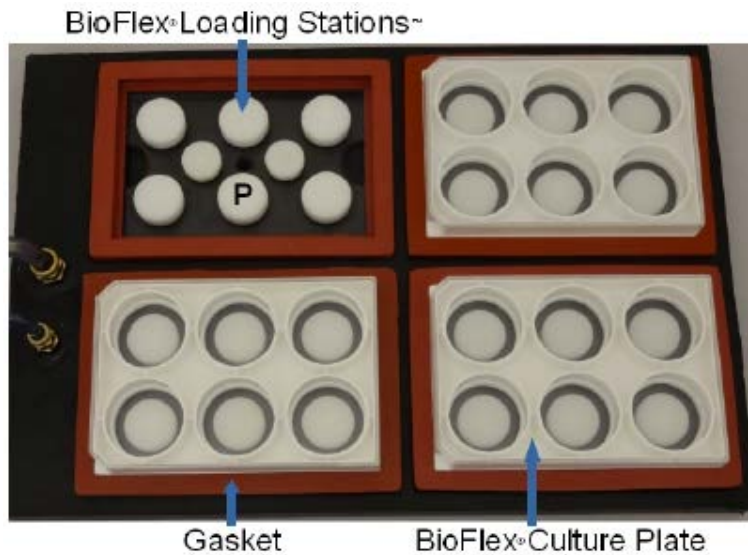


**Fig.9: BioFlex® baseplate showing the Loading Stations™ with six loading posts (P) and BioFlex® culture plates in red, rubber gaskets**

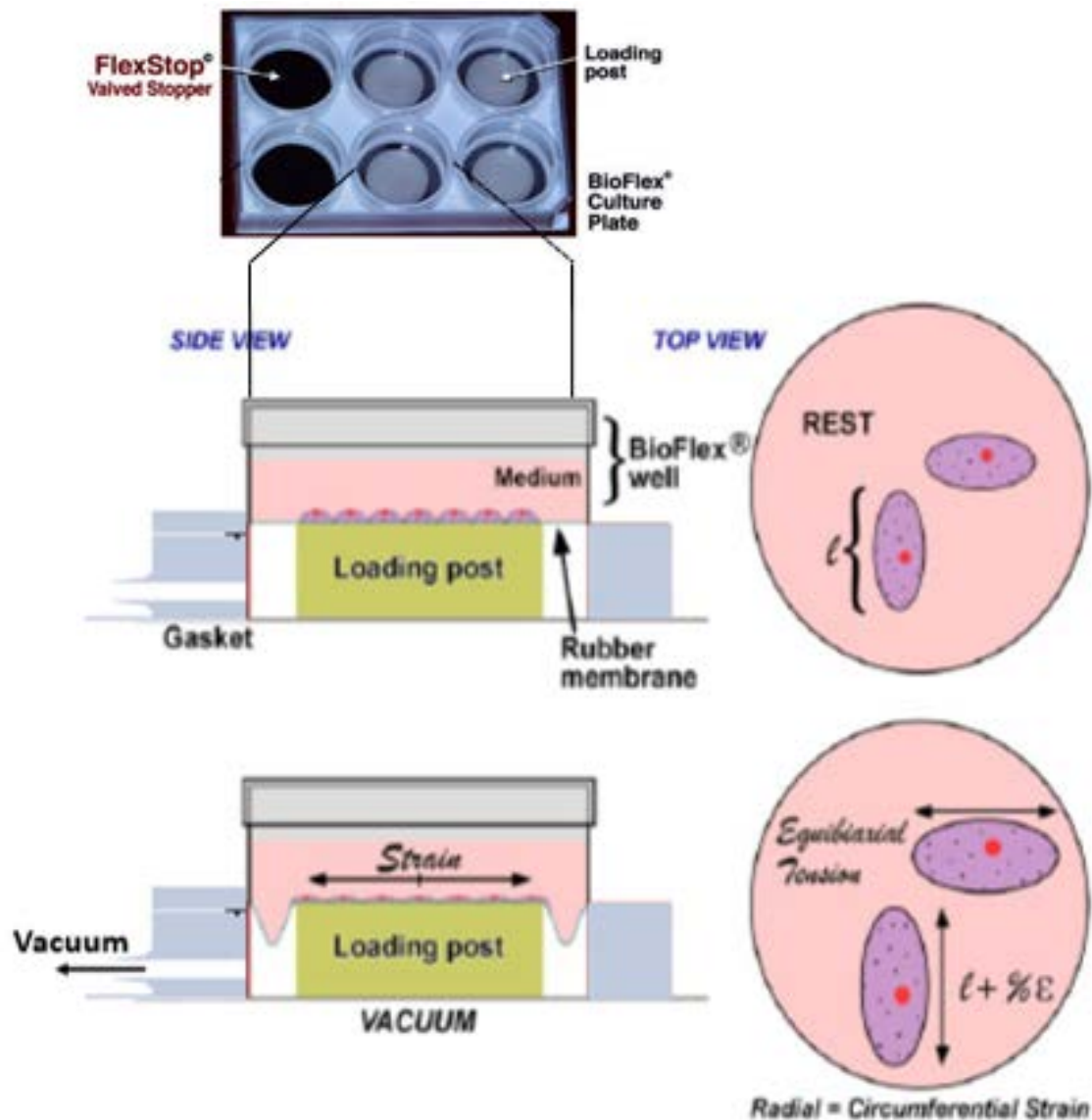


**Fig. 10: Equibiaxial strain application to cells plated on a StageFlexer® Membrane and clamped in a StageFlexer® Strain Device.**

Loading posts are available in three standard diameters: 25, 28, and 31 mm. Their use renders:

- 1) constrained distension to the flexible membrane, and
- 2) Nominal fluid shear stress because the medium is not moving up and down over the field. [49]

The loading posts of 25mm diameter, which is the most commonly used, the vacuum level predetermines the minimum and maximum strain capabilities, expressed in terms of % elongation which are 0.8% and 21.8%.

**ii. Flexible-bottomed Bioflex plates:**

Collagen I-coated flexible- silicone membrane bottomed BioFlex plates are specially designed for culturing the cells a mechanically active environment, by providing radial and circumferential strains when used on the loading posts in the Flexcell system. The Flexible silicone elastic membranes are covalently bonded with Collagen I. The growth surface area is 9.62 cm<sup>2</sup>/well, in each well of the six-well plate. These plates are feasible to work with fluorescent probes or immunohistochemical assays, as they have low autofluorescence and are optically clear for direct viewing of cells with inverted or upright microscopes (membrane thickness: 0.020 inch).

**iii. Flexcell® Tension system**

FX-5000T Flexercell Tension Plus system is a computer regulated bioreactor that uses vacuum pressure, regulated by state-of –the-art digital valve to robotically maintain and regulate vacuum pressure that would deform flexible bottomed culture plates, thereby providing specified strain regimen:

It is equipped with a 25-mm BioFlex loading station designed to provide uniform radial and circumferential strain across a membrane surface along all radii. BioFlex loading station is composed of a single plate and six planar 25-mm cylinders per plate centered beneath each well of the BioFlex plate, and the top surface is just below the BioFlex membrane surface. [49]

The silicone membranes with cultured cells were then placed on a vacuum manifold situated in an incubator. Each BioFlex membrane is stretched over the post when under vacuum pressure, creating a single-plane uniformly stretched circle:

When a precise vacuum was applied to the bottoms, controlled by a computer, the silicone membranes were deformed to a prearranged elongation percentage and returned to their original conformation once the vacuum was released. After this procedure, the cells remain adherent, and the deformation of the membrane is directly transmitted to the cells. With a 25-mm loading post and Bioflex Plates, the system provides approximate equibiaxial extension in the central region of the membrane above the post and provides biaxial strain that has a major part in the radial and a minor one in the circumferential direction within the periphery membrane field away from the post [39, 40].

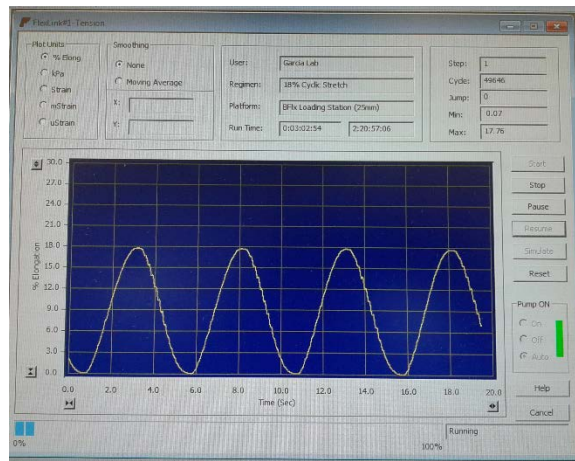


**Fig. 11: Waveform plot showing typical sinusoidal waveform.**

The radial and circumferential strain was experimentally determined by the vendor (Flexcell International) by stamping the BioFlex membrane with a dot pattern followed by labeling the distance between each pair of dots and measuring their change relative to vacuum levels. Experimental measurements demonstrated that the part of the membrane stretching over the post (25-mm diameter) received uniform strain in the radial direction that was proportional to vacuum level [41].

## 2.. EXPERIMENTAL PROCEDURES

### *IN VITRO*

All experiments using animals were previously approved by the Institutional Animal Care and Use Committee at the University of Illinois at Chicago. The animals were maintained as per the University of Illinois protocol for animal use. The studies reported here adhere to the principles outlined by the Animal Welfare Act and the National Institutes of Health guidelines for the care and use of animals in biomedical research.

#### 1. Generation of wild type and heterozygous/homozygous mice

##### **S1P Lyase wild type and heterozygous mice:**

Wild type mice (*Sgpl<sup>+/+</sup>*) and S1PL heterozygous (*Sgpl<sup>+/-</sup>*) in 129SV background and were obtained from Dr. Philip Soriano (Seattle) and were bred and housed in a specific pathogen-free barrier facility maintained by University of Illinois at Chicago Animal Resources Center.

##### **Genotyping:**

The mice were genotyped by multiplex PCR of tail snip DNA using three primers:

5'-CGCTCAGAAGGCTCTGAGTCATGG-3',

5'-CATCAAGGAAACCCTGGACTACTG-3', and

5'-CCAAGTGTACCTGCTAAGTTCCAG-3'.

The following conditions were used: denaturation, 94 °C for 5 min; amplification, 94 °C for 1 min, 58 °C for 1 min, 72 °C for 1 min (40 cycles); extension, 72 °C for 1 min. The wild-type *Sgpl1* gene fragment is ~300 bp in length, and the mutant *Sgpl1* gene fragment is ~600 bp in length. This would distinguish *Sgpl1<sup>+/+</sup>* mice from *Sgpl1<sup>+/-</sup>*

### **SphK1 wild type and knock out mice:**

*Sphk1*<sup>-/-</sup> were obtained from Dr. Richard L. Proia (NIH, Bethesda, MD) and were backcrossed to C57BL/6 background for two generations (F2 hybrid). The resultant mixed background of C57BL/6 strain and the original background (F2 hybrid) were used as controls and are referred to hereafter as wild type (WT).

### **2. Mechanical ventilation:**

Tracheotomy was performed, and the trachea was cannulated with a 20-G intravenous catheter through the mouth. Ventilation was performed at 30 ml/kg tidal volume, 0 PEEP for 4 hours at the rate of 75 breaths per minute. Non-ventilated animals were used as controls. The mice received boluses 0.1 ml/hr of phosphate buffered saline (PBS) to maintain arterial blood pressure in the normal range. <sup>4</sup>

Animals were euthanized, a median sternotomy was performed, and perfusion of the lungs was done by injection of calcium and magnesium-free PBS through the right ventricle of the heart, to clear the pulmonary intravascular space. The lungs were harvested, snap-frozen and later stored at -80°C, until further analysis.

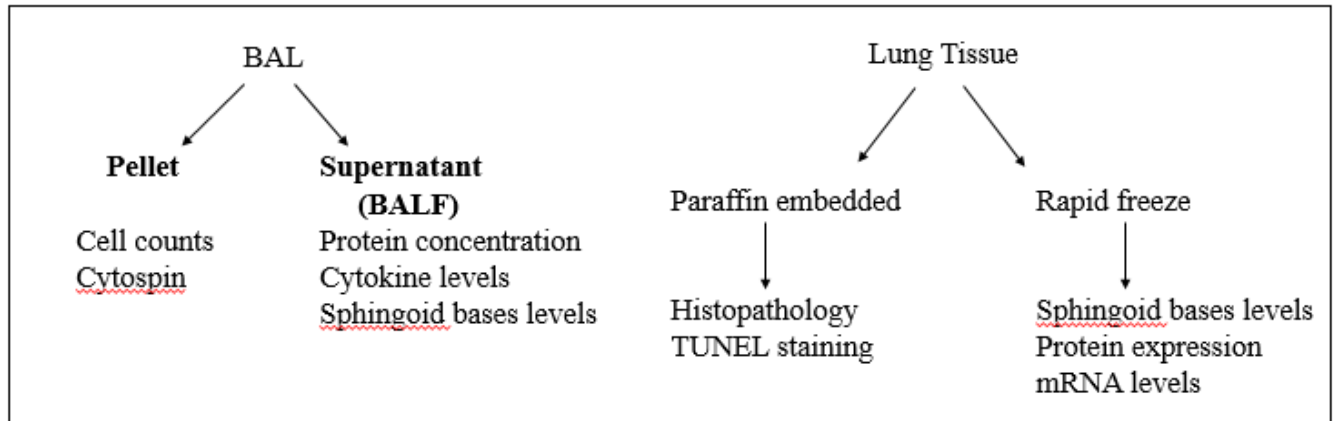


**Fig.12: Schema showing the analysis of VILI.**

### **3. BAL Collection and quantitative measures of VILI**

Bronchoalveolar lavage (BALF) collection with PBS was undertaken as follows: 1 ml of PBS with 0.1% bovine serum albumin was injected into the airway through tracheal catheter, then gently aspirated. The collected lavage fluid was centrifuged at 500g for 20 minutes at 4°C. The supernatant was centrifuged at 9600g for 10 min at +4°C. The resultant supernatant, termed the BALF was removed and frozen at -80°C for further analysis. Cell pellets from initial centrifugation were resuspended in 200µl PBS and total cell counts were determined using a hemocytometer. Aliquots were spun onto microscope slides and stained for differential cell counts.

Lung inflammation was measured by evaluating the differential cell counts in the BALF, using Diff-Quik stain set (Dade-Behring, Newark, DE). The number of macrophages and neutrophils were enumerated. Cytokine levels in the cell-free BAL samples were measured using ELISA kits (Peprotech, NJ), according to the manufacturer's instructions. Levels of active IL-6 were quantified.

The lung injury, in terms of alveolar permeability, was evaluated by measuring the protein concentrations in BAL fluid using the BCA protein assay kit (Pierce Thermo scientific, Rockford, IL). Optical density readings of samples were converted to milligrams/milliliters, using values

obtained from a standard curve generated with 0.1 to 2 mg/mL serial dilutions of bovine serum albumin.

#### **4. Lung Tissue harvesting and analysis:**

The lungs were excised, rapidly frozen in liquid nitrogen and stored at -80°C. Pieces of lung tissue were homogenized, and whole tissue lysates were prepared for further analysis. RNA was isolated from frozen lungs using TRIZOL reagent (Life Technologies, Grand Island, NY) according to the manufacturer's instructions. Portion of the lung tissue and BALF were also used for the measurement of sphingoid bases by Mass Spectrometry.

- a. Electrospray ionization liquid chromatography tandem mass spectrometry for analysis of Sphingoid Bases, Sphingoid Base 1-Phosphates, Sphingosine and Ceramides**—Analyses of the sphingolipids in the lung tissue and BALF were performed by combined LC/MS/MS on 4000 Q-trap hybrid triple quadrupole linear ion trap mass spectrometer (Applied Biosystems, Foster City, CA) equipped with a TurboIonSpray ionization source interfaced with an automated Agilent 1100 series liquid chromatograph and autosampler (Agilent Technologies, Wilmington, DE). The sphingolipids were ionized via electrospray ionization (ESI) with detection via multiple reaction monitoring (MRM). Analysis of sphingoid bases and the molecular species of ceramides used ESI in positive ions with MRM analysis. Briefly resolution of sphingoid bases was achieved with a Discovery C<sub>18</sub> column (2.1 × 50 mm, 5-µm particle size; Supelco, Bellefonte, PA) and a gradient from methanol/water/formic acid (61:38:1, v/v) with 5 mM ammonium formate to methanol/acetonitrile/formic acid (39:60:1, v/v) with 5 mM ammonium formate at a flow rate of 0.5 ml/min. The MRM transitions used for detection of sphingoid bases were as

follows:  $m/z$  286  $\rightarrow$  268 (C<sub>17</sub>-Sph, internal standard),  $m/z$  300  $\rightarrow$  282 (Sph), and  $m/z$  302  $\rightarrow$  284 (DHSph).

Ceramide molecular species were resolved using a 3  $\times$  100-mm X-Terra XDB-C<sub>8</sub> column (3.5- $\mu$ m particle size; Waters, Milford, MA) and a gradient from methanol/water/formic acid (61:39:0.5, v/v) with 5 mM ammonium formate to acetonitrile/chloroform/water/formic acid (90:10:0.5:0.5, v/v) with 5 mM ammonium formate at a flow rate of 0.5 ml/min. MRM transitions monitored for the elution of ceramide molecular species were as follows:  $m/z$  510  $\rightarrow$  264, 14:0-Cer;  $m/z$  538  $\rightarrow$  264, 16:0-Cer;  $m/z$  540  $\rightarrow$  284, 16:0-DHCer;  $m/z$  552  $\rightarrow$  264, 17:0-Cer (internal standard);  $m/z$  564  $\rightarrow$  264, 18:1-Cer;  $m/z$  566  $\rightarrow$  284, 18:1-DHCer;  $m/z$  566  $\rightarrow$  264, 18:0-Cer;  $m/z$  568  $\rightarrow$  284, 18:0-DHCer;  $m/z$  594  $\rightarrow$  264, 20:0-Cer;  $m/z$  596  $\rightarrow$  284, 20:0-DHCer;  $m/z$  624  $\rightarrow$  284, 22:0-DHCer;  $m/z$  650  $\rightarrow$  264, 24:1-Cer;  $m/z$  652  $\rightarrow$  284, 24:1-DHCer;  $m/z$  652  $\rightarrow$  264, 24:0-Cer;  $m/z$  654  $\rightarrow$  284, 24:0-DHCer;  $m/z$  680  $\rightarrow$  264, 26:1-Cer;  $m/z$  682  $\rightarrow$  264, 26:0-Cer;  $m/z$  708  $\rightarrow$  264, 28:1-Cer; and  $m/z$  710  $\rightarrow$  264, 28:0-Cer.

S1P and DHS1P were quantified as bisacetylated derivatives with C<sub>17</sub>-S1P as the internal standard using reverse-phase high pressure liquid chromatography separation, negative ion ESI, and MRM analysis. Standard curves for each of the sphingoid bases, sphingoid base 1-phosphates, ceramide molecular species, were constructed via the addition of increasing concentrations of the individual analyte to 30 pmol of the structural analogs of the sphingolipid classes used as the internal standards. Linearity and the correlation coefficients of the standard curves were obtained via a linear regression analysis. The standard curves were linear over the range of 0.0–300 pmol of each of the sphingolipid analytes with correlation coefficients ( $R^2$ ) > 0.98.

### **b. Western Blotting:**

The lung tissue was dissected with clean tools, on ice preferably, and rapidly frozen to prevent degradation by proteases. Small fraction of the lung tissue was suspended in ~200ul of lysis buffer along with protease and phosphatase inhibitors and homogenized with an electric homogenizer. The sample was then sonicated and centrifuged at 10,000g at 4°C for 10 minutes. The supernatant was collected into fresh tubes on ice and the total protein concentration was determined by BCA protein assay (Pierce Chemical, Rockford, IL) for equal protein loading. The lung tissue lysates with equal protein concentration were boiled with 6X lamelli buffer for five minutes. Cell lysates (30 µg/lane) were separated by SDS polyacrylamide gel electrophoresis (PAGE) on a 10% pre-cast gel run at constant voltage (125 V) and transferred to nitrocellulose membranes (Bio-Rad, Hercules, CA) in transfer buffer (Novex). The membrane was incubated for 1h at room temperature in blocking buffer (Tris-buffered saline + Tween 20 with 1% BSA) to reduce non-specific binding. The membrane was then incubated with the respective primary antibody S1P Lyase (Santa Cruz), SphK1 (AbCam) and SphK2 (AbCam) overnight. After four 10-min washes with TBST, the membrane was incubated (1 h) with the respective secondary antibody in TBST with 1% BSA. The membrane was rinsed again four times with TBST, and the bands were detected using Supersignal luminol enhancer (Perbio Science UK Ltd., Cheshire, UK) followed by exposure on blue-light-sensitive film (Hyperfilm; Amersham Biosciences UK Limited, Little Chalfont, UK).

Equal protein loading was verified by re-probing membranes with anti-β-actin antibody. The relative intensities of protein bands (relative density units) were quantified by scanning densitometry using ImageJ software (Molecular Dynamics, Sunnyvale, CA).

**c. RNA isolation and RT-PCR:**

Total RNA was isolated from mouse lung homogenate using TRIzol reagent (Life Technologies, Grand Island, NY), according to the manufacturer's instructions. iQ SYBR Green Supermix (Life Technologies) was used to perform real-time PCR using iCycler by Bio-Rad.

GAPDH (sense) 5'-GGTCCTCAGTGTAGCCCAAG-3';  
and (antisense), 5'-TGCCCAGAACATCATCCCT-3' was used as an external control to normalize expression. Quantitative RT-PCR was performed as previously described. All primers were designed by inspection of the genes of interest and were designed using Beacon Designer software version 2.1 (Premier Biosoft, Palo Alto, CA). The sequence descriptions of mouse primers used are as follows:

Mouse SphK1: 5'-GCTGTCAGGCTGGTGTATG-3' (forward) and  
5'-ATATGCTTGCCCTTCTGCAT-3' (reverse);

Mouse SphK2, 5'-ACTGCTCGCT-TCTTCTCTGC-3' (forward) and  
5'-CCACTGACAGGAAGGAAAA- 3' (reverse);

Mouse Sgp11, 5'-AACTCTGCCTGCTCAGGGTA-3' (forward) and  
5'-CTCCTGAGGCTTCCCTTCT-3' (reverse);

Negative controls, consisting of reaction mixtures containing all components except target RNA, were included with each of the real-time PCR runs. To verify that amplified products were derived from mRNA and did not represent genomic DNA contamination, representative PCR mixtures for each gene were run in the absence of the reverse transcriptase enzyme after first being cycled to 95°C for 15 minutes.

Amplicon expression in each sample was normalized to GAPDH content. Analysis of results and fold differences were determined using the comparative CT method. Fold change was calculated using a comparative quantification algorithm from the  $\Delta\Delta C_t$  values with the formula

( $2^{-\Delta\Delta Ct}$ ), and data are presented as relative to the endogenous normalizer GAPDH mRNA expression.

#### **d. Lung Histology Analysis**

After washing with fresh PBS, fixed tissues were dehydrated, cleared, and embedded in paraffin by routine methods. The lungs were then removed en bloc, fixed to pressure (15-cm water) with neutral-buffered 2% paraformaldehyde overnight, embedded in paraffin, divided into sections (5 mm thick), and stained with H&E at the Research Histology Laboratory (Department of Pathology, University of Illinois at Chicago).<sup>3</sup> Sections (5 mm) were collected on Superfrost Plus positively charged microscope slides (Fisher Scientific Co., Houston, TX), deparaffinized, and stained with hemotoxylin and eosin.

#### **e. TUNEL Assay**

End labeling of exposed 3'-OH ends of DNA fragments was undertaken with the TUNEL in situ cell death detection kit Alkaline Phosphatase (Roche Diagnostics, Indianapolis, IN), as per the manufacturer's instructions. At least two sections were used from each mice for analyses.

### ***IN VITRO***

#### **Cell culture:**

Mouse transformed lung epithelial cells (MLE-12 cells) were cultured in DMEM complete medium (5% FBS, 100 U/mL penicillin, and streptomycin) at 37°C and 5% CO<sub>2</sub>. They were allowed to grow to approximately 90% confluence, as characterized by typical cobblestone morphology. Cells from T-75 flasks were detached with 0.05% trypsin, suspended in fresh complete medium, and seeded at standard densities ( $8 \times 10^5$  cells/well) onto collagen I-coated

flexible- silicone membrane bottomed BioFlex plates (V Flexcell International, Hillsborough, NC). Both static and cells exposed to different magnitudes of cyclic stretch (5% and 18%) were seeded onto identical plates and placed in the same cell culture incubator to ensure standard culture conditions. All CS experiments were performed in the presence of complete culture medium.

## **5. Cyclic stretch:**

Cyclic stretch experiments were performed with the FX-5000T Flexercell Tension Plus system (Flexcell International, McKeesport, PA). After the cells attained 80% confluence, the media was replenished and two hours later, they were mounted onto the Flexercell Tension Plus system (FX-5000T, Flexcell International). Cells were then subjected to different regimens and exposed to sinusoidal cyclic stretch of desired magnitude (5 or 18% elongation) for 48 hours. The 18% linear elongation with equibiaxial stretch (0.2 Hz, 25 cycles/min, sinusoidal wave) was high magnitude cyclic stretch reprising the mechanical stretch underwent by the alveolar epithelium during high tidal volume ventilation, whereas 5% simulates physiological conditions.

### **5.a Lipid Extraction and Sample Preparation for LC/MS/MS for analysis of Sphingoid bases:**

Cellular lipids were extracted by a modified Bligh and Dyer procedure with the use of 0.1N HCl for phase separation. C17-S1P (40 pmol) was employed as internal standard, and was added during the initial step of lipid extraction. The extracted lipids were dissolved in methanol/chloroform (2:1, v/v), and aliquots were taken to determine the total phospholipid content as described. Samples were concentrated under a stream of nitrogen, re-dissolved in methanol, transferred to auto sampler vials, and subjected to S1P-DHS1P LC/MS/MS analysis. Details of the method are mentioned above.

### **5.b Western Blotting:**

MLE-12 cells were cultured in cyclic stretch six-well plates and subjected to cyclic stretch of 5% and 18% for 48-hours. After 48-hours, the cells were washed with PBS and lysed with 75ul lysis buffer containing protease and phosphatase inhibitors. The cell lysates were sonicated and the total protein contents were determined by the BCA protein assay (Pierce Chemical, Rockford, IL). The cell lysates with equal protein concentration were boiled with 6X lamelli buffer for five minutes. Cell lysates (25 µg/lane) were separated by SDS polyacrylamide gel electrophoresis (PAGE) on a 4-20% gel or a 10% pre-cast gel) run at constant voltage (125 V) and transferred to nitrocellulose membranes (Bio-Rad, Hercules, CA) in transfer buffer (Novex). Membranes were incubated for 1h at room temperature in blocking buffer (Tris-buffered saline + Tween 20 with 1% BSA) to reduce nonspecific binding. The membrane was then incubated overnight with the primary antibody S1P Lyase (Santa Cruz), SphK1 (AbCam) and SphK2. After three 10-min washes with TBST, the membrane was incubated (1 h) with the respective secondary antibody in TBST with 1% BSA. The membrane was rinsed, and bands were detected using Supersignal luminol enhancer (Perbio Science UK Ltd., Cheshire, UK) followed by exposure on blue-light-sensitive film (Hyperfilm; Amersham Biosciences UK Limited, Little Chalfont, UK). Bands were quantified using densitometry (Leica Q600S; Quantimet 6,000 v01.06A, Leica Microsystems Inc., Chantilly).

Equal protein loading was verified by re-probing of membranes with anti- $\beta$ -actin antibody. The relative intensities of protein bands (relative density units) were quantified by scanning densitometry using ImageJ software (Molecular Dynamics, Sunnyvale, CA). Densitometry results were expressed as a ratio of specific protein signal to  $\beta$ - actin signal. Protein density was normalized by the unstretched control density.

### 5.c RNA isolation and RT-PCR:

Total RNA was isolated from mouse lung homogenate using TRIzol reagent (Life Technologies, Grand Island, NY), according to the manufacturer's instructions. iQ SYBR Green Supermix (Life Technologies) was used to perform real-time PCR using iCycler by Bio-Rad.

Quantitative RT-PCR was performed as previously described. All primers were designed by inspection of the genes of interest and were designed using Beacon Designer software version 2.1 (Premier Biosoft, Palo Alto, CA). The sequence descriptions of mouse primers used are as follows:

Mouse SphK1: 5`-GCTGTCAGGCTGGTGTATG-3` (forward) and  
5`-ATATGCTTGCCCTTCTGCAT-3` (reverse);

Mouse SphK2: 5`-ACTGCTCGCT-TCTTCTCTGC-3` (forward) and  
5`-CCACTGACAGGAAGGAAAA- 3` (reverse);

Mouse Sgpl1: 5`-AACTCTGCCTGCTCAGGGTA-3` (forward) and  
5`-CTCCTGAGGCTTTCCCTTCT-3` (reverse);

18S RNA (sense, 5`-GTAACCCGTTGAACCCATT-3`; and  
antisense, 5`-CCATCCAATCGGTAGTAGCG-3`)

18S RNA was used as an external control to normalize expression. Negative controls, consisting of reaction mixtures containing all components except target RNA, were included with each of the real-time PCR runs. To verify that amplified products were derived from mRNA and did not represent genomic DNA contamination, representative PCR mixtures for each gene were run in the absence of the reverse transcriptase enzyme after first being cycled to 95°C for 15 minutes. In the absence of reverse transcription, no PCR products were observed.

Amplicon expression in each sample was normalized to 18S RNA content. Analysis of results and fold differences were determined using the comparative CT method. Fold change was

calculated using a comparative quantification algorithm from the  $\Delta\Delta C_t$  values with the formula  $(2^{-\Delta\Delta C_t})$ , and data are presented as relative to the endogenous normalizer 18S mRNA expression.

## **6. Immunofluorescence:**

The elastic bottom of the BioFlex plates were excised with a scalpel and transferred to a polystyrene 6-well cell culture plate. Each membrane was covered with 2ml PBS. Small portions of the membrane were cut and the pieces placed in a 96-well plate. MLE-12 cells subjected to cyclic stretch were washed three times with PBS and then fixed with 3.7% paraformaldehyde in PBS for 10 min at room temperature. After they had been washed three times with PBS, the cells were permeabilized with 0.5% Triton X-100 in PBS for 10 min, rinsed with PBS, and blocked with 1% bovine serum albumin for 30 min. The elastic membranes of the wells with the cells were excised into 12-well dishes for staining.

The cells were then immunostained with primary antibodies as indicated for 1 h at room temperature. After they had been washed three times with TBST, the cells were incubated with FITC-conjugated phalloidin for 1 h and then stained with DAPI for nuclei. The coverslips were mounted in anti-fade solution, and images were taken with the confocal microscope.

Following immunostaining, the elastic membranes of the wells with cells were mounted onto large coverslips and then the slides were examined under a Nikon Eclipse TE 2000-S fluorescence microscope (Tokyo, Japan) with a Hamamatsu digital charge-coupled device camera (Hamamatsu, Japan) using a 20X objective lens and MetaVue software version 1.0 (Universal Imaging Corp, Downingtown, PA). All images were acquired randomly with 40X objective with consistent intensity setting.

## **7. Flow Cytometry analysis for apoptosis:**

Apoptosis, driven by high amplitude cyclic stretch can be enumerated by flow cytometry. The cells were co-stained with FITC- Annexin V (25 ng/ml; green fluorescence) and Propidium Iodide (dye

exclusion, red fluorescence), following manufacturer's instructions (BD BioSciences) and was analyzed by flow cytometry (Beckman Coulter Co, USA). Briefly, the cells subjected to cyclic stretch were rinsed with PBS and detached from the plates using 1ml cell stripper solution. The cells were suspended in binding buffer at  $3 \times 10^5$  cells/100  $\mu$ l, supplemented with 5 $\mu$ l of FITC-Annexin-V and incubated for 15 min at room temperature in the dark. 3 $\mu$ l of PI was conjugated and finally the cells were suspended in 400  $\mu$ l 1X binding buffer. The cell were sorted by flow cytometer. Flow cytometric analysis was performed with a FACScan Xow cytometer (Becton–Dickinson, San Jose, CA). Comparative experiments were performed at the same time by bivariate flow cytometry using a FACScan (BD) and analyzed with CellQuest software on data obtained from the cell population from which debris was gated out.

## 2. RESULTS

### IN VIVO

We used rodent models to investigate the effect of mechanical ventilation.

WT 129SV mice, were subjected to normal breathing (control) or ventilator-assisted breathing (VILI) at 0 PEEP, 30ml/kg tidal volume for 4 hours. The whole lungs were lavaged and BAL fluids were collected and right lung was embedded in formalin and the remaining lung tissue was rapidly frozen. The whole lung tissue was processed accordingly to be used for measuring the sphingolipid levels, protein expression and measuring the mRNA levels.

#### 1. Expression of sphingoid bases and sphingolipids metabolizing enzymes

##### after VILI:

##### i. Levels of sphingoid bases in mouse lung and BALF after VILI

Analysis of lung tissue and BALF from WT mice subjected to ventilation for sphingolipid levels by LC-MS/MS revealed a significant decrease in the S1P levels, whereas a significant increase in the ceramide levels in the lung tissue was observed, when compared to animals with spontaneous breathing, as shown in Fig 13. No change in sphingosine level was noted between the two groups.

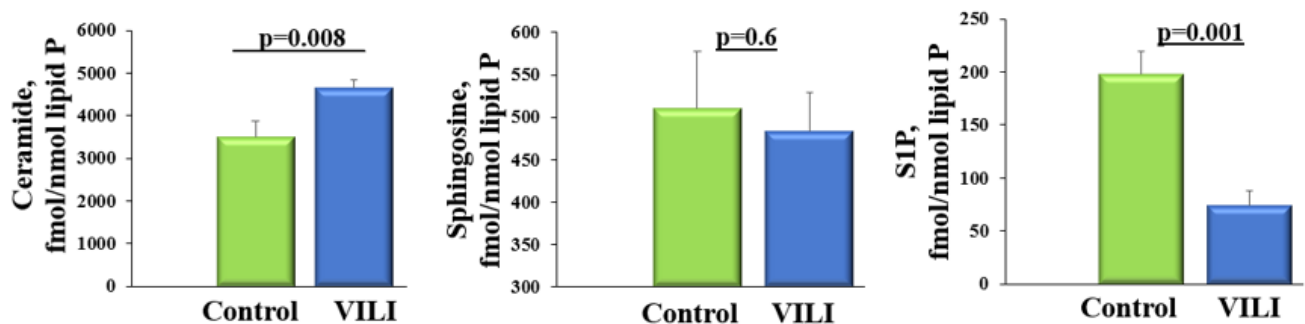
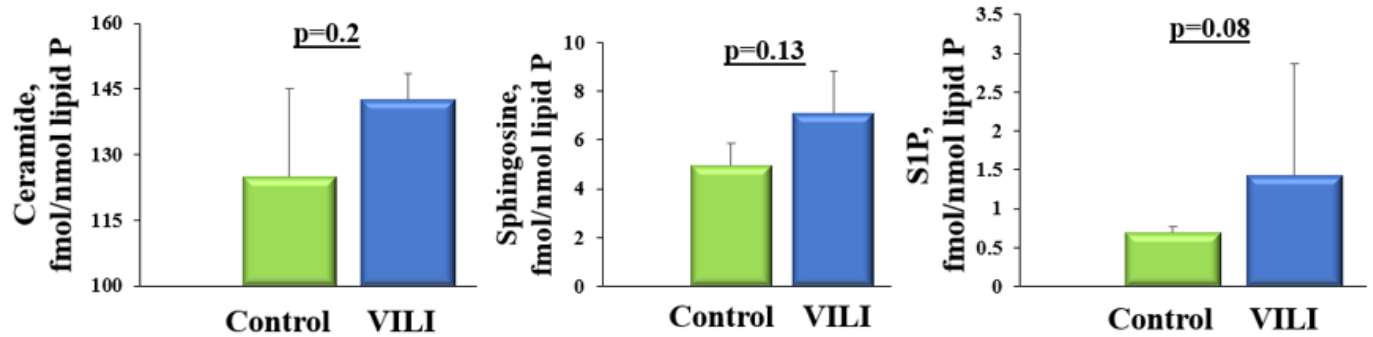


Fig. 13: Levels of sphingoid bases in mouse lung after VILI

In contrast to mouse lung, no change in S1P, ceramide and sphingosine levels was observed in BALF from control and VILI mice, as shown in Fig. 14.



*Fig. 14: Levels of sphingoid bases in BALF after VILI*

**ii. Expression of sphingolipid metabolizing enzymes in mouse lung after VILI:**

The relative protein expression levels of SphK 1 and 2 and S1PLyase in lung tissues from animals subjected to spontaneous breathing and animals subjected to mechanical ventilation, were determined by Western blotting, as shown in Fig. 15.

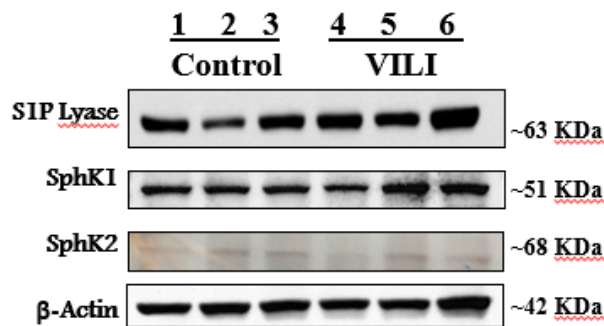


*Fig 15: Expression of S1P Lyase, SphK1, SphK2 and actin in mouse lung after VILI.*

Whole lung homogenates were subjected to SDS-PAGE and it was observed that Sgpl1 and SphK1 levels were significantly elevated in lung tissues of ventilated mice compared to control animals. SphK2 protein expression, however, remained unaltered in response to ventilation. There

was some discrepancy between protein and mRNA levels. Mechanical ventilation resulted in a decreased mRNA expression of S1P Lyase, SphK1 and SphK2, as shown in Figure 16.

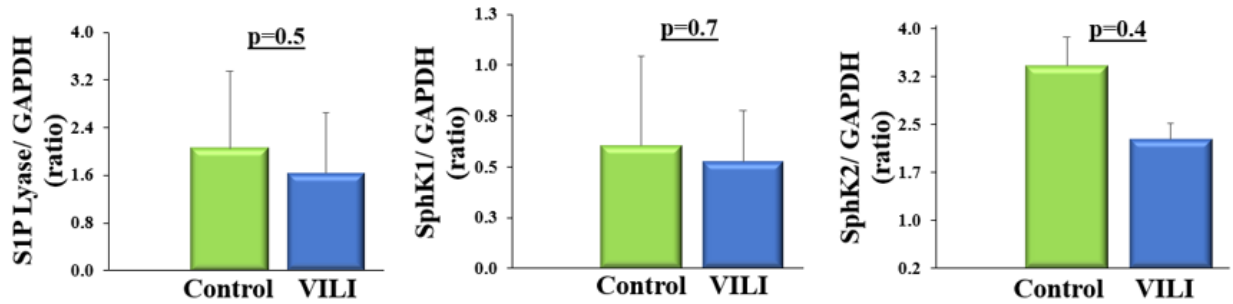


**Fig. 16: mRNA levels of S1PLYase, SphK1 and SphK2 and in mouse lung after VILI.**

These results suggests that mechanical ventilation alters ceramide and S1P levels as well as the expression of S1P Lyase enzyme and SphK1 involved in S1P metabolism.

### iii. Expression of S1P Lyase in BALF after VILI

Analysis of the protein expression of the sphingolipid metabolizing enzymes in the BALF from WT mice exposed to the ventilation revealed a two-fold increase in S1P Lyase protein expression, as shown in Fig. 17.

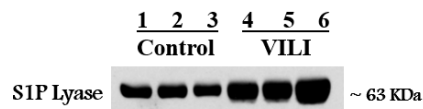


**Fig 17: Western blots of BALF after VILI probed with anti-S1P lyase Antibody.**

On the other hand, SphK1 and SphK2 protein expression was not observed in BALF from ventilated and control mice (data not shown). This clearly unveils the vital role of S1P Lyase in ventilator induced lung injury.

As VILI modulated S1PLYase expression, we investigated the role of S1P Lyase in ventilator induced lung injury by using 129SV background wild type and *Sgpl1*<sup>+/-</sup> mice.

## 2. Role of sphingolipid metabolizing enzymes in VILI

*Sgpl1*<sup>+/-</sup> mice do not survive for more than six weeks after birth as they exhibit vascular defects [42]. Hence, we used the *Sgpl1*<sup>+/-</sup> (heterozygous) mice wherein there was partial restoration of the S1P Lyase activity, which was sufficient to protect from organ damage.

After three weeks of birth, the mice were genotyped. The wild-type *Sgpl1* gene fragment is ~300 bp in length, and the mutant *Sgpl1* gene fragment is ~600 bp in length, as shown from Figure 18.



**Fig. 18: Genotyping for *Sgpl1*<sup>+/+</sup> and *Sgpl1*<sup>+/-</sup> mice**

Analysis by LC-MS/MS revealed a small but significant increase of S1P levels in lung tissue and BAL fluids, but not in plasma of *Sgpl1*<sup>+/-</sup> mice, as compared with WT mice, as shown in Fig 19A. S1PL mRNA in *Sgpl1*<sup>+/-</sup> mice were approximately 50% of WT mice, as shown in Fig 19B. A reduction in S1PL activity of lung homogenates from *Sgpl1*<sup>+/-</sup> mice. [43]

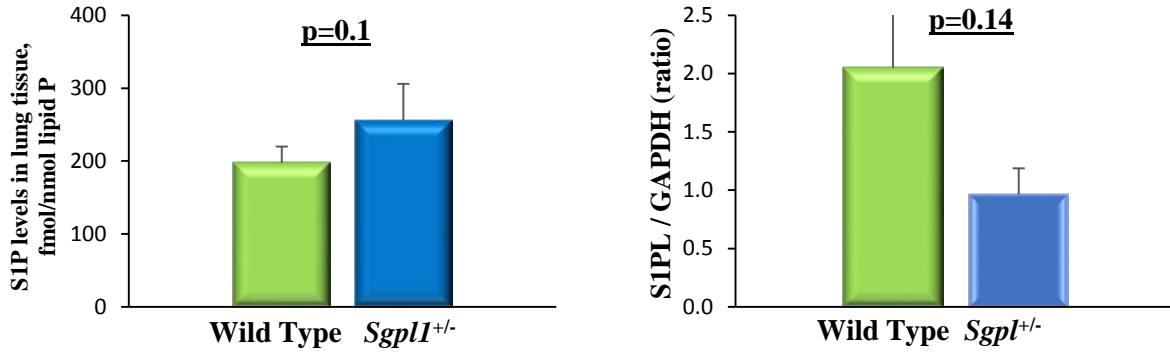
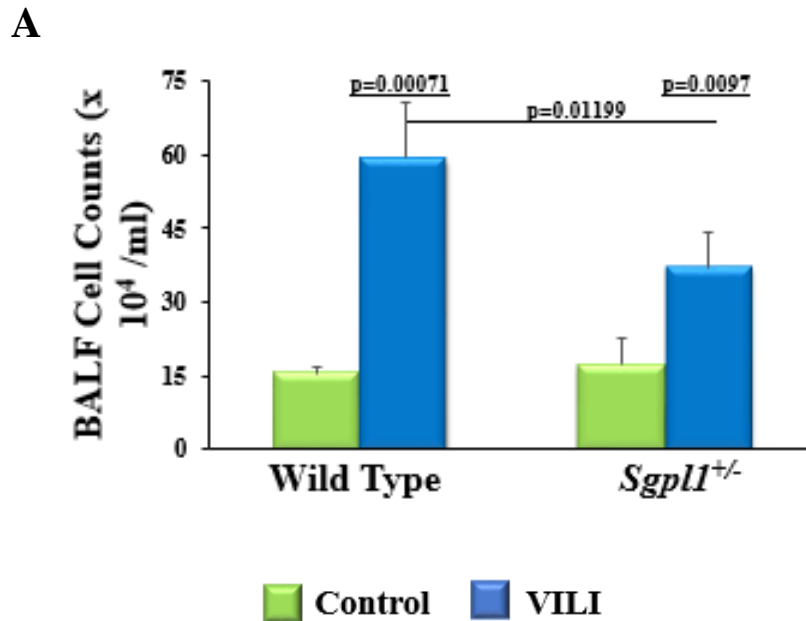


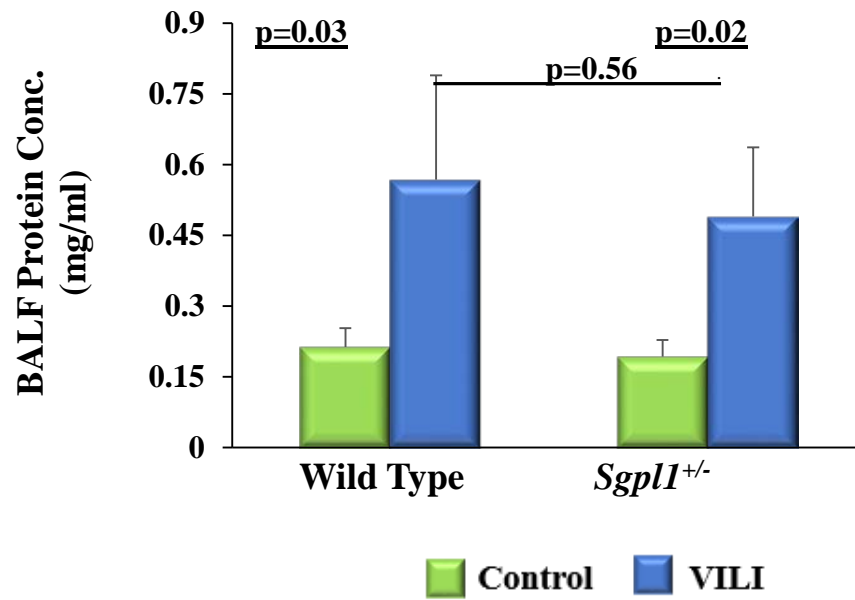
**Fig.19: A. S1P levels of wild type and *Sgpl1*<sup>+/-</sup> mice B. mRNA levels of wild type and *Sgpl1*<sup>+/-</sup> mice.**

**i. Assessment of VILI in wild type and *Sgpl1*<sup>+/-</sup> mice:**

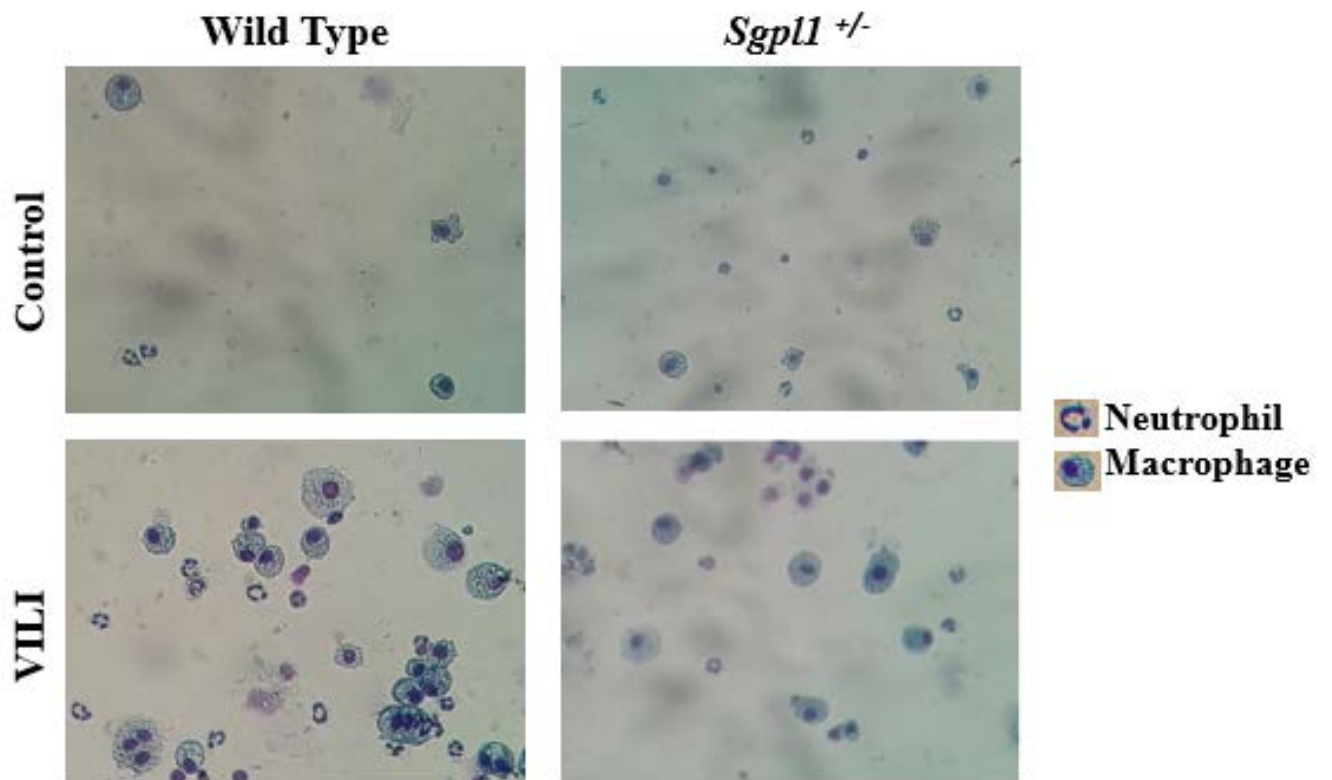
To assess whether S1PL plays a role in ventilator-induced lung injury, control WT and *Sgpl1*<sup>+/-</sup> mice were subjected to ventilation under the same conditions as described above. Analysis of BALF from WT mice exposed to the ventilation demonstrated significantly greater inflammation and injury compared to that from animals in the control groups, as shown in Fig. 20.



**B**



**C**



D

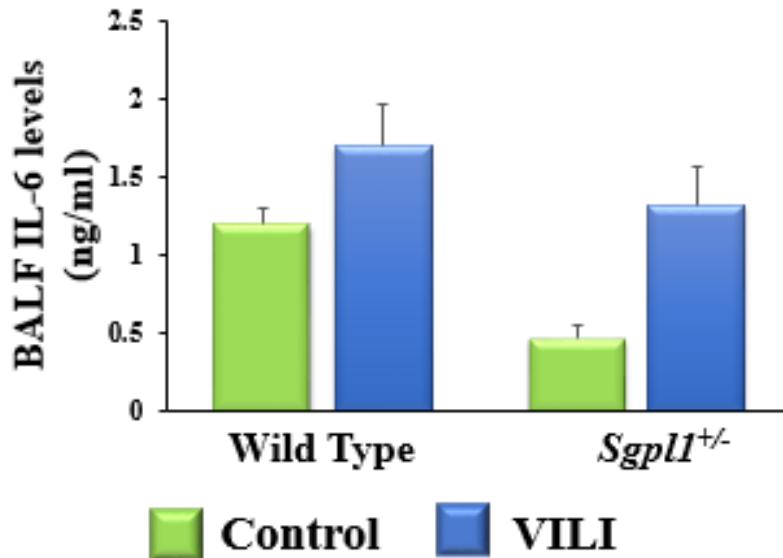


**Fig.20: Assessment of VILI in WT and *Sgpl1*<sup>+/-</sup> mice**

BAL from wild type mice exposed to the model of ventilator induced lung injury showed significantly higher total cell counts (Fig. 20A), total protein (Fig. 20B); and infiltration of neutrophils and macrophages (Fig. 20C), compared to that from *Sgpl1*<sup>+/-</sup> mice. BAL levels of IL-6 in animals exposed to the ventilation model were significantly higher than those in the VILI in *Sgpl1*<sup>+/-</sup> groups, as shown in Fig 20 D.

ii. **Alveolar infiltration in wild type and *Sgpl1*<sup>+/-</sup> mice after VILI:**

Using hematoxylin and eosin staining, no significant differences in lung morphology between WT and *Sgpl1*<sup>+/-</sup> controls were observed; however, influx of inflammatory cells into alveolar space and injury in response to mechanical ventilation was attenuated in *Sgpl1*<sup>+/-</sup> mice compared with WT mice (Figure 21).

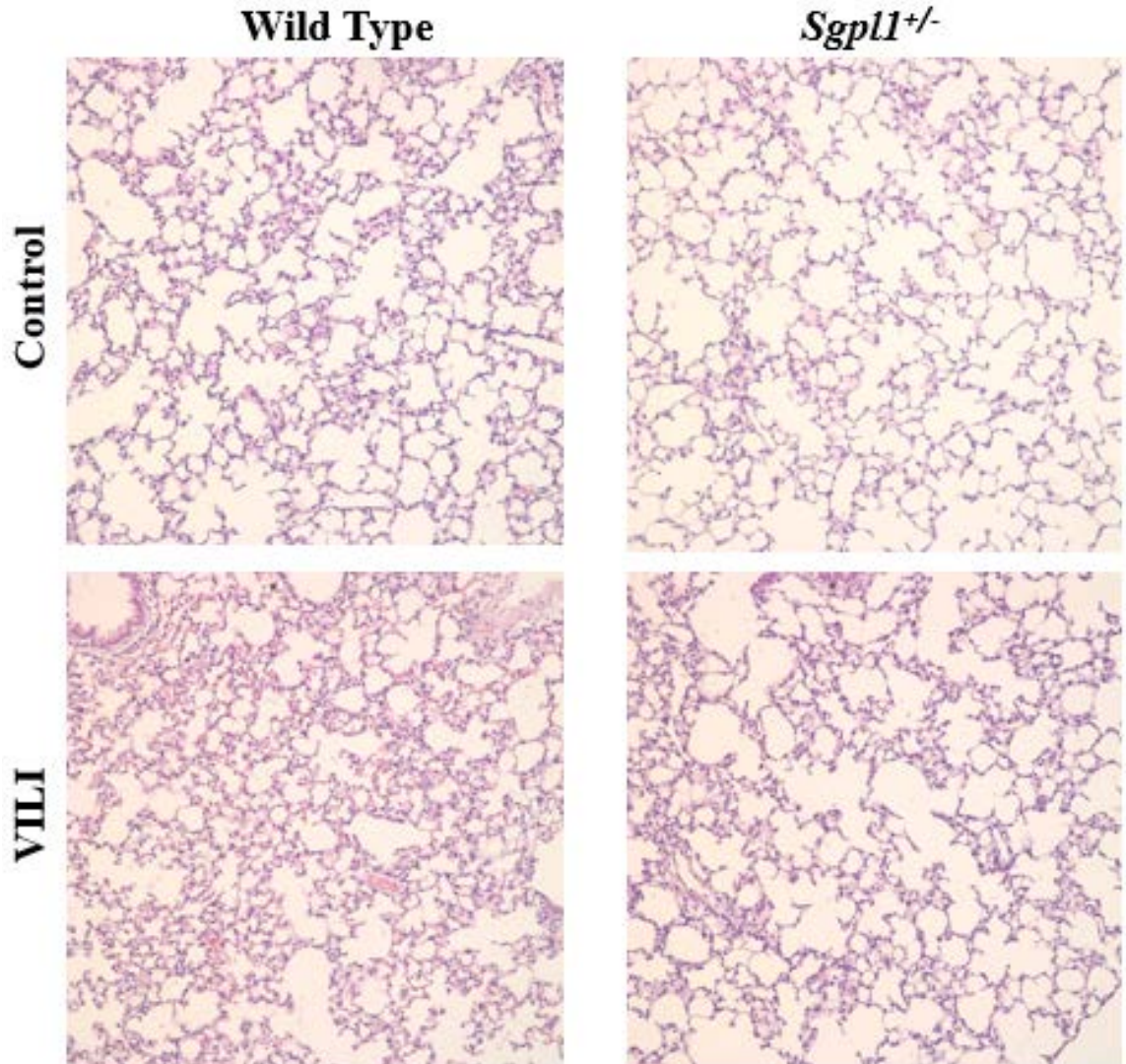


**Fig 21: Alveolar infiltration after VILI in wild type and *Sgpl1*<sup>+/-</sup> mice**

iii. **TUNEL positive cells after VILI in wild type and *Sgpl1*<sup>+/-</sup> mice:**

DNA fragmentation is a hallmark of apoptosis. Single-stranded/ double stranded breaks during DNA cleavage can be detected by labelling the free ends with modified nucleotides like fluorescein-dUTP, whose polymerization is catalyzed by the deoxynucleotidyl transferase (TdT). This TUNEL (TdT-mediated dUTP-X nick end labeling) was used to quantify the cellular apoptosis caused due to the ventilator induced lung injury was estimated by TUNEL. TUNEL

staining was done on the lung sections from mice after termination of the mechanical ventilation.

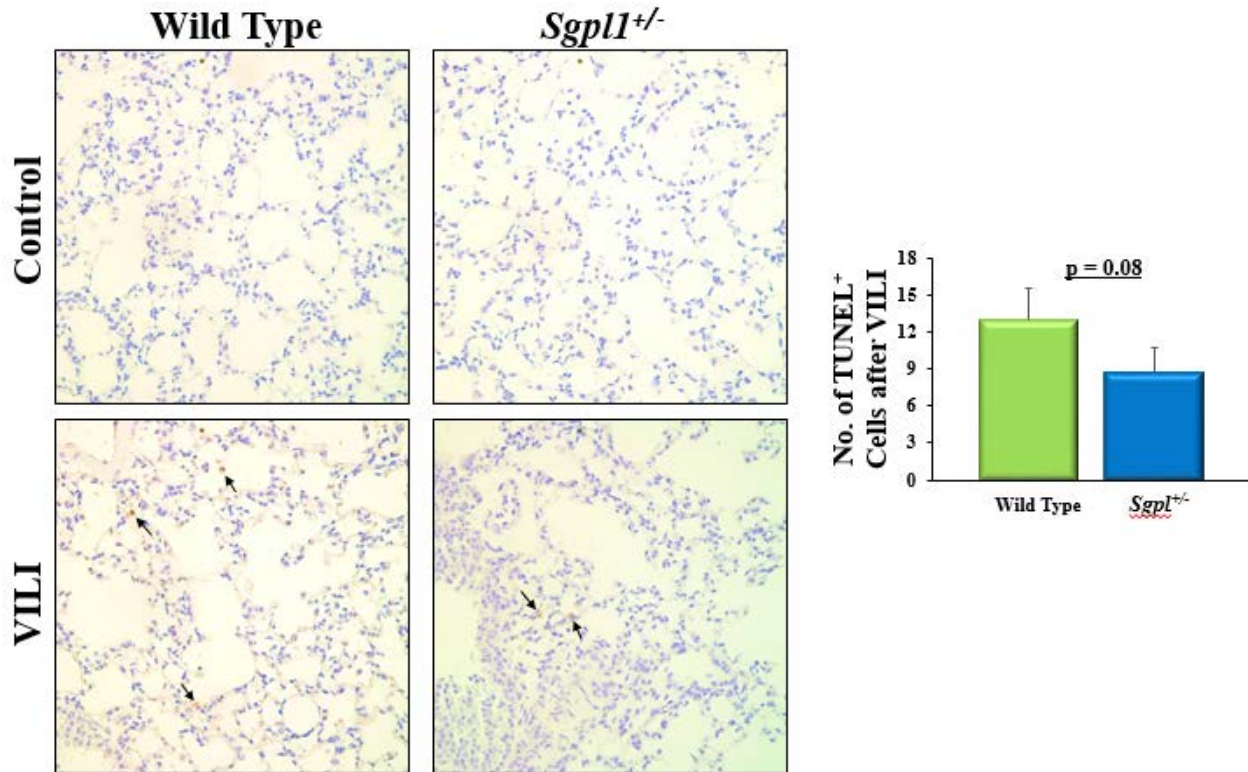


**Fig 22: TUNEL Positive cells in WT and *Sgpl1*<sup>+/-</sup> mice after VILI**

Mechanical ventilation induced increase in terminal deoxynucleotidyl transferase dUTP nick end labelling (TUNEL)<sup>+</sup> cells was attenuated in *Sgpl1*<sup>+/-</sup> mice, when compared to mechanically ventilated wild type mice, as shown in Fig. 22. The mean numbers of TUNEL<sup>+</sup> cells per high-power field 6 SEM in lung sections of WT and *Sgpl1*<sup>+/-</sup> mice is quantitated.

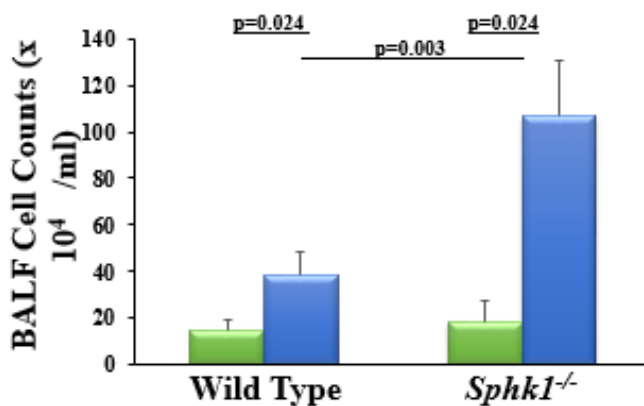
Together these finding suggest the pathophysiological contribution of S1P Lyase to acute lung injury. The *Sgpl1*<sup>+/-</sup> mice are genetically programmed for deletion of single *Sgpl1* allele that modulates S1P levels in lung tissue and BAL fluids, and partially protects mice against ventilator-induced lung injury.

iv. Assessment of VILI in C57B WT and *Sphk1*<sup>-/-</sup> mice:

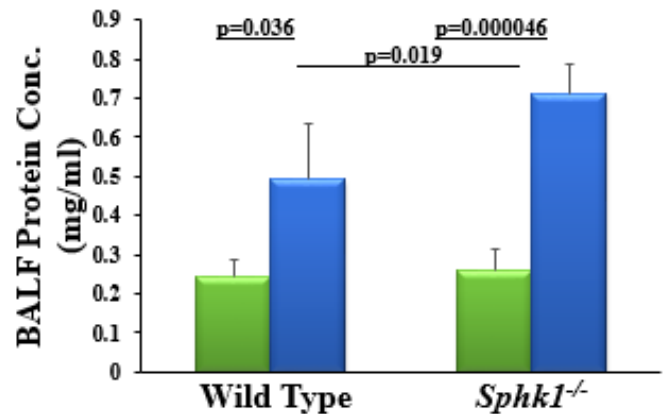
S1P accumulated in the cells is a balance between its synthesis catalyzed by SphK1 and SphK2 and catabolism mediated by S1P phosphatases and S1P Lyase. In this study we determined the effect of knock down of SphK1 on VILI. WT (C57BL/6J) and *Sphk1*<sup>-/-</sup> mice were exposed to ventilation for 4 hours at 0 PEEP and 30ml/kg tidal volume. Later, the mice were euthanized, lungs were lavaged by PBS solution, and BAL fluids were analyzed as described in Materials and Methods.

Deficiency of SphK1 resulted in an increase in pulmonary vascular leak after ventilation, as significantly shown by higher total cell counts (Fig. 23.A), increase in BAL fluid protein concentration (Fig. 23 B), and increased neutrophils and macrophages (Fig. 23 C) in *Sphk1*<sup>-/-</sup> mice compared with WT mice subjected to ventilation.

A



B



 Control  VILI

C

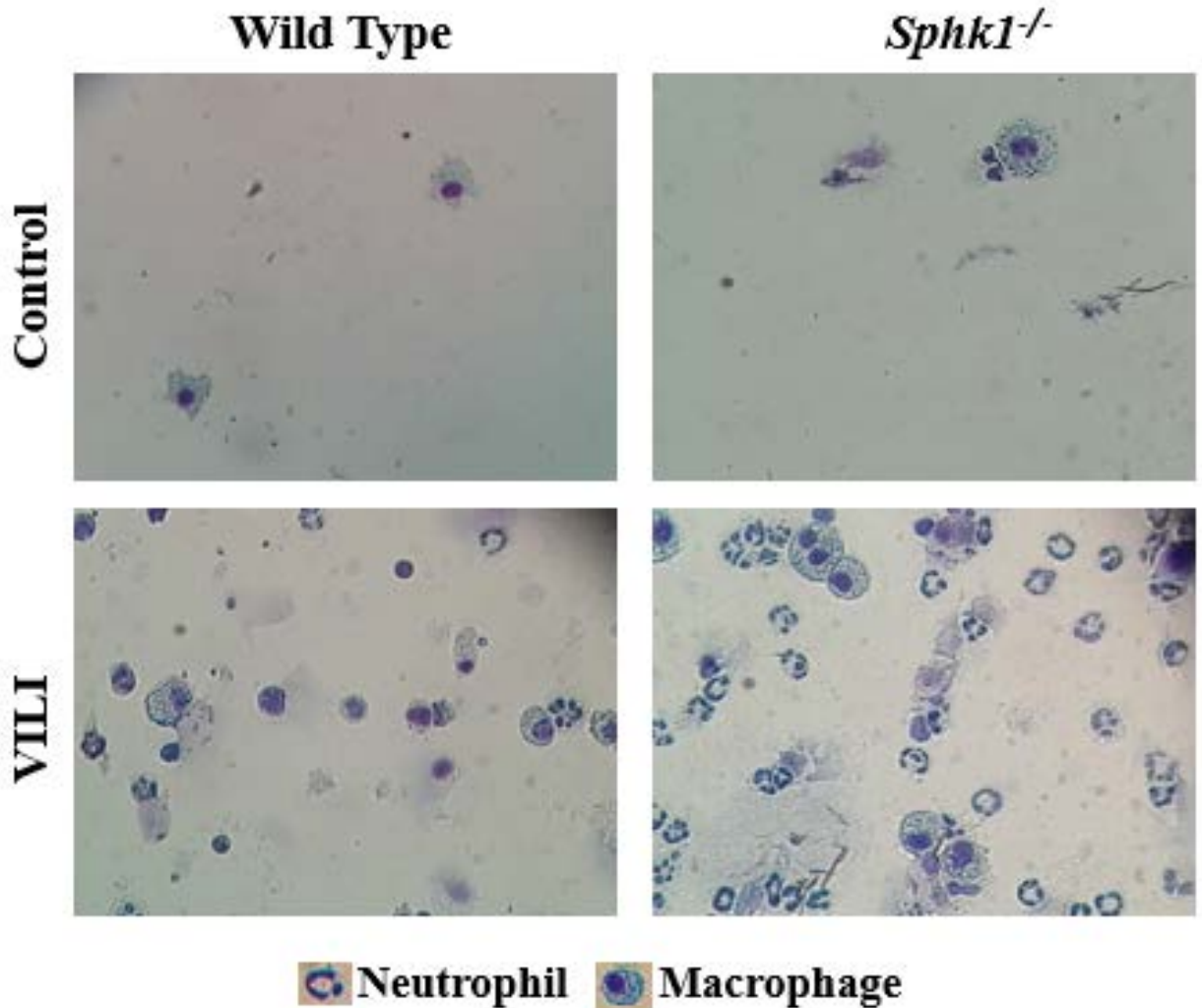


**Fig.23: Assessment of VILI in WT and *Sphk1*<sup>-/-</sup> mice**

v. **Alveolar infiltration after VILI in wild type and *Sphk1*<sup>-/-</sup> mice:**

Using hematoxylin and eosin staining, no significant differences in lung morphology between WT and *Sphk1*<sup>-/-</sup> controls were observed; however, influx of inflammatory cells into alveolar space and injury in response to mechanical ventilation was found to be higher in *Sphk1*<sup>-/-</sup> mice compared with WT mice (Figure 24).

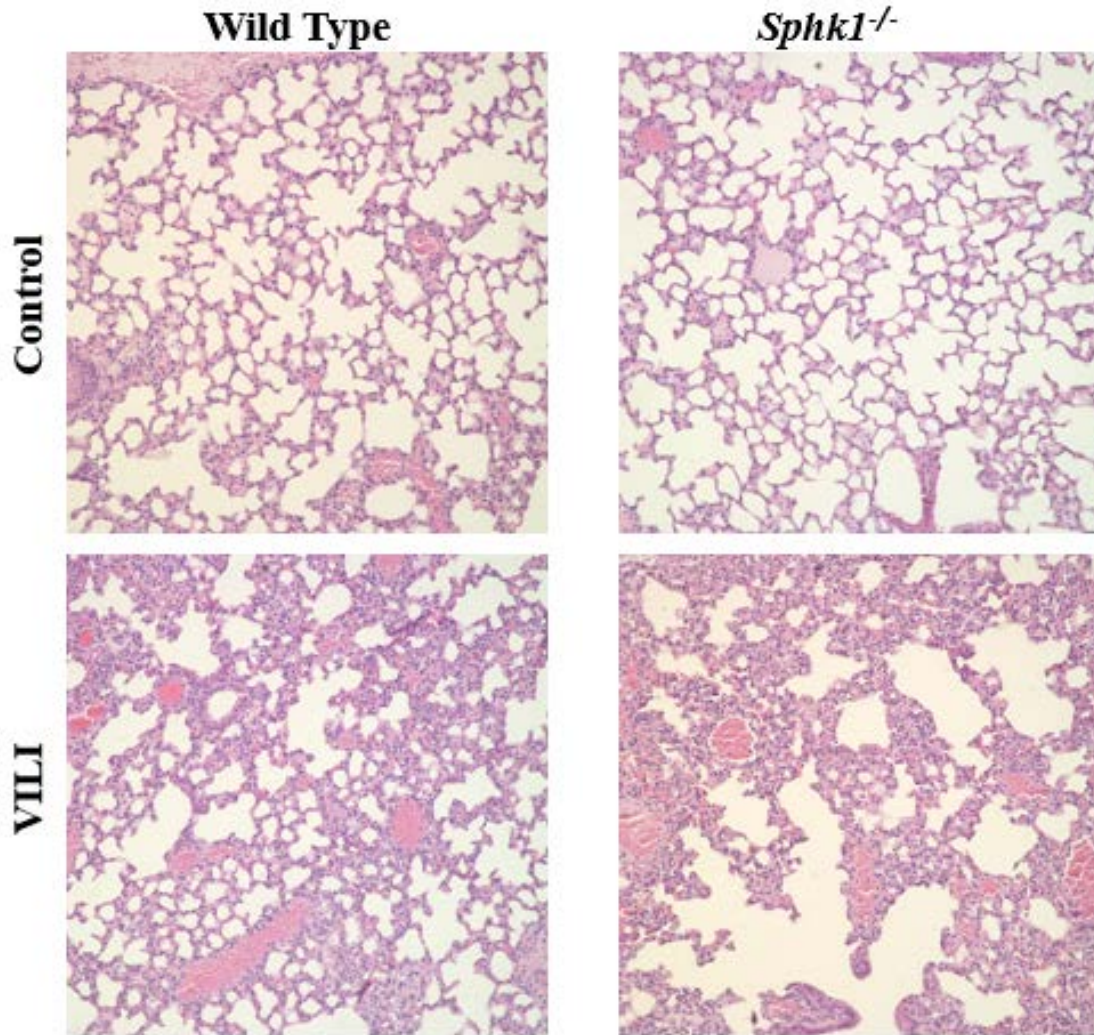


**Fig24: Alveolar infiltration after VILI in wild type and *Sphk1*<sup>-/-</sup> mice.**

Deficiency of *Sphk1* resulted in exacerbation of VILI. Together these findings suggest a vital role of SphK1/S1P signaling in maintaining lung homeostasis. The *Sphk1*<sup>-/-</sup> mice are genetically programmed for deletion of *Sphk1* allele, which resulted in severe injury due to mechanical ventilation.

## ***IN VITRO***

Having established the role of S1P Lyase *in vivo*, the expression of S1P Lyase after cyclic stretch of MLE-12 and HLMVEC was studied.

### **3. Expression of sphingoid bases and sphingolipids metabolizing enzymes in MLE-12 to cyclic stretch.**

#### **i. Expression of S1P Lyase in epithelial and endothelial cells after cyclic stretch:**

Cyclic stretch was found to increase S1P Lyase expression in human lung microvascular endothelial cells (HLMVECs) and mouse lung epithelial cells (MLE-12 cells) after 48-hours of 18% equibiaxial cyclic stretch on the cells, as shown in Fig 25.

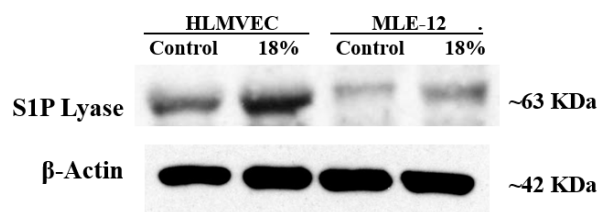


**Fig. 25: S1P Lyase expression after 18% cyclic stretch**

#### **ii. Expression levels of sphingoid bases, S1P Lyase in MLE-12 cells after physiological and pathophysiological conditions of cyclic stretch:**

The 18% linear elongation with equibiaxial stretch (0.2 Hz, 25 cycles/min, sinusoidal wave) was high magnitude cyclic stretch represents the mechanical stretch underwent by the alveolar epithelium during high tidal volume ventilation, whereas 5% simulates physiological conditions. MLE-12 cells were simultaneously subjected to 5% and 18% stretch with a static plate as control.

In the whole cell lysates, S1P Lyase protein expression was elevated in cells after prolonged 18% cyclic stretch for 48-hours. There was discrepancy between protein and mRNA levels. Prolonged 18% cyclic stretch for 48-hours, as the S1P Lyase mRNA levels went lowered.

Analysis of sphingoid base levels by LC-MS/MS in MLE-cells subjected to different magnitudes of cyclic stretch revealed a significant decrease in the S1P levels and also sphingosine levels, whereas a significant increase in the ceramide levels in the MLE-12 after 18% stretch, when compared static and 5% stretch, as shown in Fig 26.

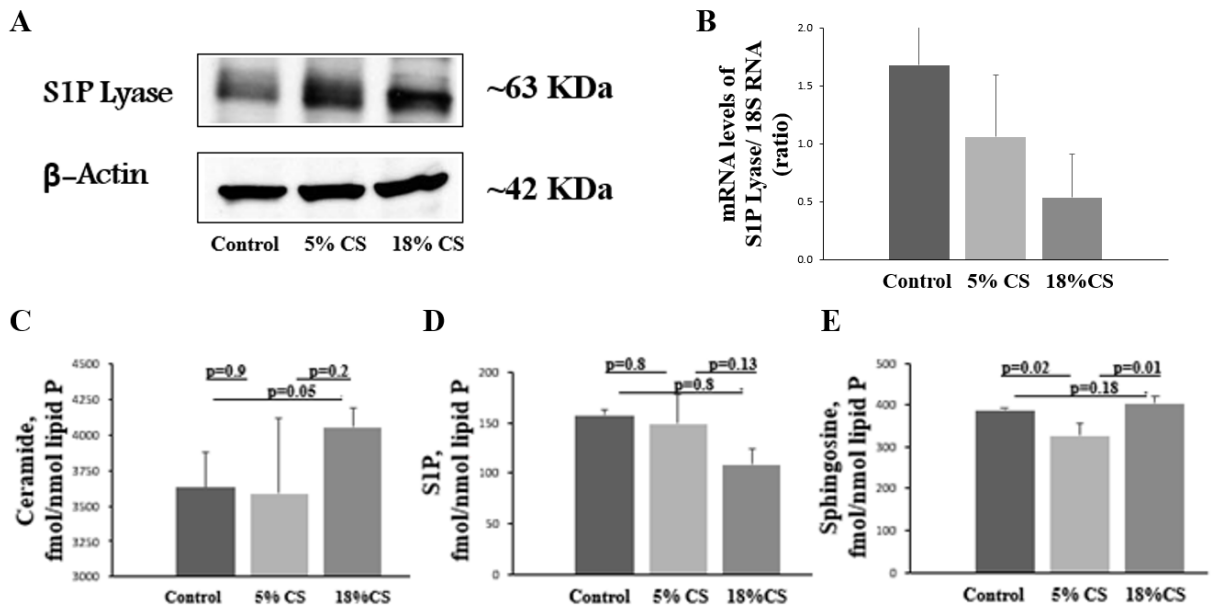


**Fig 26: Expression levels of sphingoid bases, S1P Lyase in MLE-12 cells after cyclic stretch**

#### 4. Effects of CS on cell apoptosis:

##### i. **Biochemical Markers of apoptosis**

Caspases are the most critical molecules for the execution of apoptosis, out of which Caspase-3, once activated executes apoptosis by cleaving a variety of substrates, or “death substrates”. Activation of caspase-3 results in the cleavage of the 34KDa into activated 17KDa and 12KDa fragments [44]. PARP, a 116 kDa nuclear poly (ADP-ribose) polymerase, is a substrate for Caspase -3 [45]. It is a DNA repair enzyme, which when cleaved loses its activity and alleviates cellular disassembly. During the cleavage of PARP, the carboxy-terminal catalytic domain (~89 kDa) is separated from the amino-terminal DNA binding domain (~24 kDa) [46]. The detection of

~89 kDa PARP fragment with Anti-PARP thus serves as an early marker of apoptosis. Cell lysates from MLE-12 cells subjected to cyclic stretch were probed for western blotting using anti-PARP and anti-Caspase antibody. The cleavage of Caspase-3 and PARP after cyclic stretch indicates apoptosis.

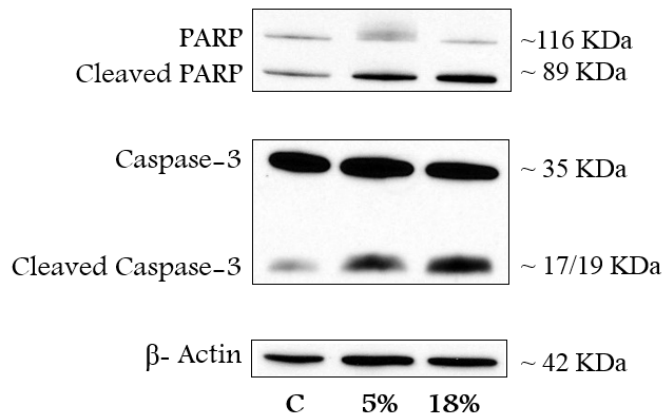


**Fig 27: Cleavage of apoptotic proteins Caspase-3 and PARP**

## ii. Flow cytometry for analysis of apoptosis

The permeability of the cell and the plasma membrane integrity of the cell during apoptosis, help us to recognize them from normal cells [47]. To confirm MLE-12 cell apoptosis, an Annexin V binding and PI staining was used for cell apoptosis analysis. Annexin V binds to the phosphatidylserine on the cell membrane, which flips outside during cell membrane damage. PI is permeable only through the membranes of dead cells. Viable cells are those which are negative for both Annexin V and PI (bottom left quadrant of Flow Cytometry). The cells in their early phase of the apoptotic process bind to Annexin V but are PI-negative (bottom right quadrant of Flow figure).

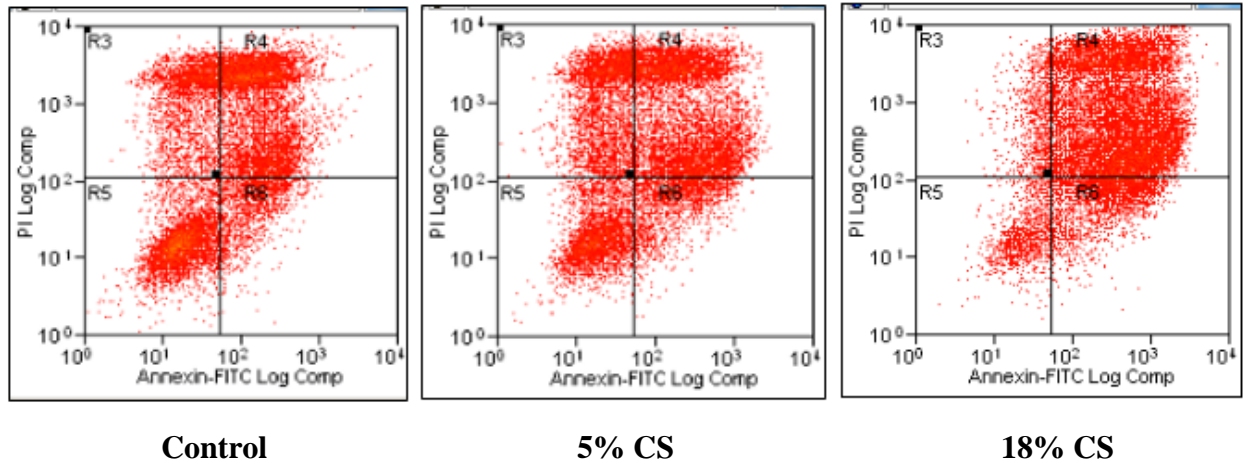


**Fig28: MLE-12 cells incubated with Annexin V and PI.**

The cells in their late phase in apoptosis stain positive for both Annexin V and PI (top right quadrant of Flow Cytometry). A series of the representative plots of the flow cytometry analysis can be seen in Fig.28

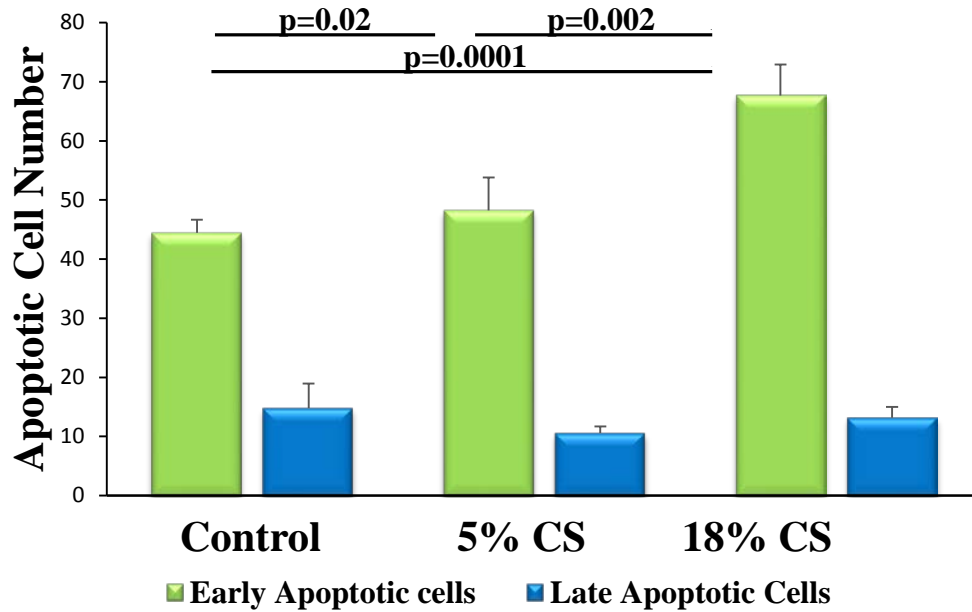


**Fig.29: Late apoptotic and early apoptotic cells after different magnitudes of cyclic stretch.**

## **5. Cell orientation after cyclic stretch:**

The cytoskeletal remodeling, visualized by the remodeling of F-actin remodeling was examined by immunofluorescence staining of F-actin in the monolayer. This would also give the extent of paracellular gap formation. MLE-12 cells exposed to 5% CS and 18% CS, were found to undergo cytoskeletal arrangement, which was ascertained and characterized by circumferential F-actin rim. Also, the central stress fibers were found to be oriented in a perpendicular direction to the main distension vector. Larger paracellular gaps were observed in 18% stretch, as shown in Fig. 30

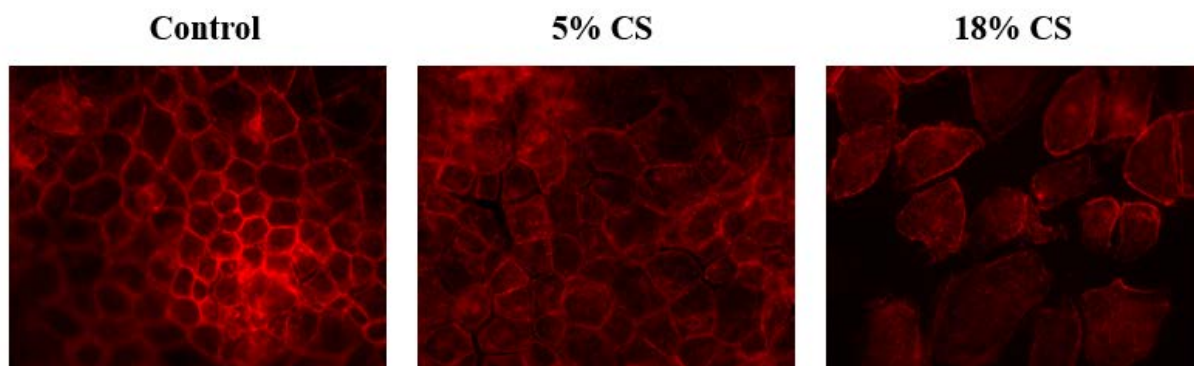


**Fig 30: Actin remodeling and gap formation after cyclic stretch.**

## **6. Effect of inhibition of S1P Lyase by 4-DP:**

### **i. Effect of 4-DP on cyclic stretch induced apoptosis:**

To determine the effect of increased S1P Lyase expression on apoptosis, cells were pretreated with a S1P Lyase inhibitor 4DP (1mM) before subjecting the cells to stretch. 4-deoxypyridoxine (DOP), inhibits S1P Lyase and all pyridoxal phosphate-dependent enzymes [48]. MLE-12 cells were treated with 4-DP (1mM) for 3 hours before cyclic stretch.

Compared to static conditions, the apoptosis was enhanced after 48 hours of 18% cyclic stretch. Pretreatment of MLE-12 cells with 4-DP, reduced apoptosis in 18% cyclic stretch cells, compared to 4-DP non-treated cells, as shown in Fig 31. These results suggest that high-magnitude CS (18%

elongation) could propagate the progressive death of alveolar epithelial cells, which was partially rescued in cells treated with 4-DP.

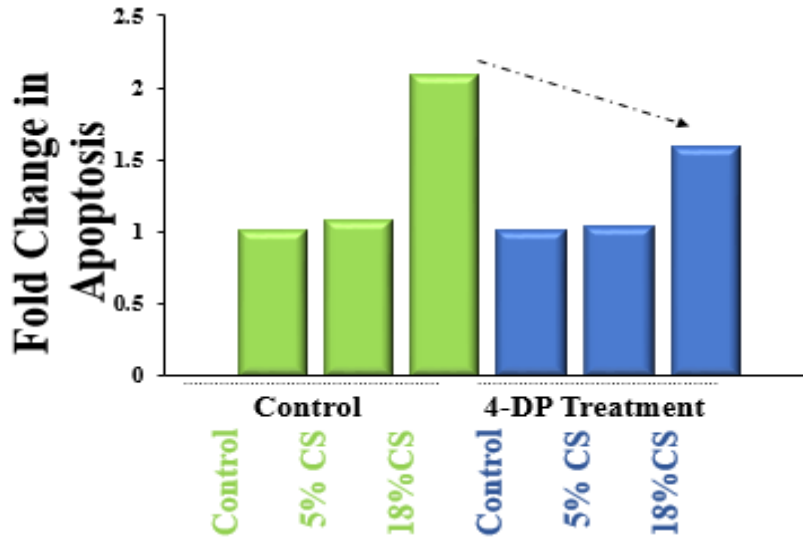


**Fig31: Effect of S1P Lyase inhibition on apoptosis**

**ii. Effect of 4-DP on paracellular gaps caused by high magnitude stretch:**

Analysis on the effect of 4-DP, showed that pre-treatment with 4-DP stimulated the closure of paracellular gaps. A dramatic reduction in the extent of paracellular gap formation was observed in cells treated with 4DP, as shown in Fig.32, The paracellular gap formation in Fig. was only observed in MLE-12 cells exposed to pathologically relevant CS levels (18% elongation) without prior 4DP treatment.

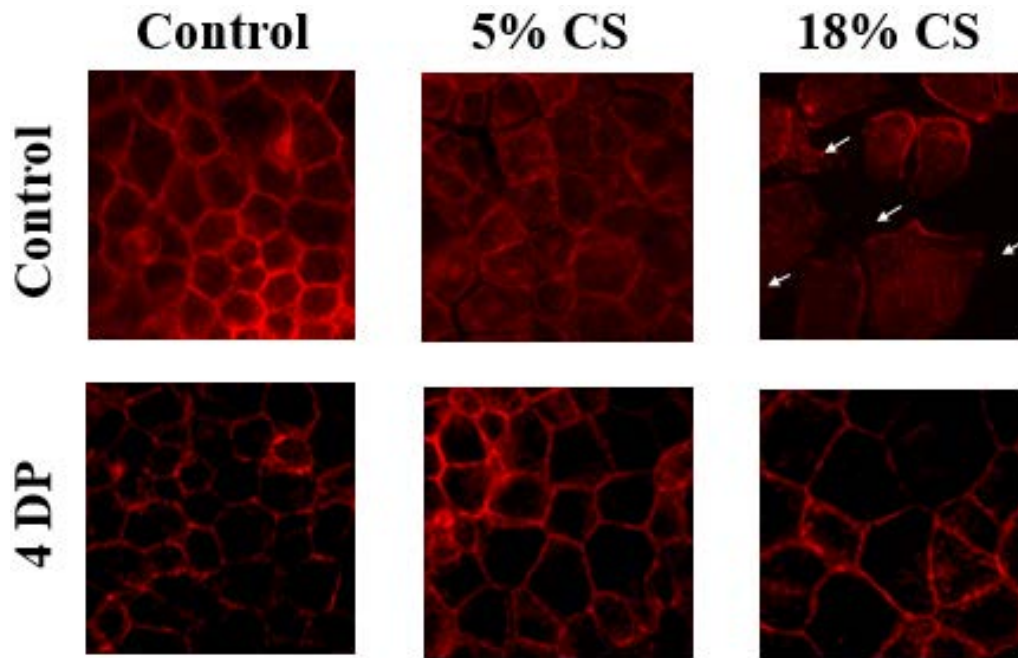


**Fig. 32: Effect of S1P Lyase inhibition on paracellular gap formation**

These results suggest the protective effects of inhibition of S1P Lyase, thereby elucidating the therapeutic potential of inhibitors of the sphingolipid metabolizing enzyme.

#### **IV. DISCUSSION**

Ventilator-induced lung injury (VILI) is a side-effect of mechanical ventilation and is a substantial problem for patients, leading to the impairment of the airway epithelium. Due to repeated collapse and reopening of the airways, the epithelium can be damaged due to a miscellanea of mechanisms. (10). The mechanical forces which often result in overstretching of the cells cause cellular deformation, apoptosis, pro-inflammatory cytokines release, plasma membrane breaks, and structural changes in tight junctions and modified protein expression.

Mechanical stimulation triggers apoptosis in the vascular system [50]. Reactive oxygen species signaling, activated by mechanical stress has a role in inducing vascular barrier dysfunction and eventually VILI [51]. VILI results in an immune response that is elicited by the fine balance between the pro-inflammatory and the anti-inflammatory cytokines. In the case of VILI, the effect of pro-inflammatory cytokines is predominant over the effect of anti-inflammatory cytokines [52]. These cytokines eventually enter the systemic circulation, resulting in multiple organ distress syndromes.

These cytokines induce alveolar leakage of proteins in a wide variety of ways by attenuating the production of surfactant in the lungs, thereby losing the surfactant function in the lung and aggravating injury [53]. Cytokines induce the activation of transcription factors, and eventually leading to recruitment of polymorphonuclear leucocytes (PMSs) and immune cells, leading to bio trauma [54].

Tremendous research has been done in elucidating the molecular mechanism causing VILI. Nonetheless there is still need to deeply explore the molecular basis of the transduction of the

mechanical forces into biochemical changes. In this study, we were the first to explore the role of sphingoid bases and sphingolipid metabolizing enzymes in VILI.

Sphingolipids elicit a plethora of cellular responses including proliferation, survival, barrier regulation, apoptosis, and inflammation. S1P synthesis requires the concerted action of ceramidase and sphingosine kinases, and once formed, S1P is either metabolized to hexadecenal and ethanolamine phosphate by the S1P Lyase or recycled to sphingosine and ceramides. The imbalance in this fine regulation of the S1P and ceramide levels has a vital role in the induction of lung injury.

In this study, we found that the mechanical ventilation differentially modulates the expression levels of the S1P-metabolizing enzymes and generation of sphingoid bases in lung tissues. During mechanical ventilation and cyclic stretch, increased expression of S1P Lyase and its activity would enhance S1P degradation resulting in reduced S1P levels in cells and tissues. Also, there is accumulation of ceramides. Therefore, blocking S1P Lyase with inhibitor(s) or activation of SphK1 should be beneficial against VILI.

Mechanical ventilation at high tidal volume was found to aggravate acute lung injury as assessed by histological changes, increased total cell counts in BAL, alveolar infiltration of neutrophils, increased capillary leakage and apoptosis. Partial knockdown of *Sgpl1* gene (*Sgpl1*<sup>+/-</sup>) offered some protection against ALI caused due to mechanical ventilation. On the other hand, knockdown of SphK1 aggravated VILI. Inhibition of S1P Lyase *in vitro* was also found to enhance barrier integrity and reduce apoptosis after mechanical stress. These results suggest that: Sphingosine-1-phosphate has a protective role in maintaining lung permeability in normal ventilation.

Thus activation of SphK1; inhibition of S1P Lyase or exogenous addition of S1P would render some protection against injury caused due to the abnormal mechanical forces acting on the lung. There are various inhibitors available, but each has its own limitations. For example, (2-acetyl-4-tetrahydroxybutylimidazole) or its analogs inhibit S1P Lyase directly as they need biotransformation. On the other hand, 4-deoxypyridoxine (4-DP) not only inhibits S1P Lyase, but also inhibits all pyridoxal phosphate dependent enzymes [55]. So, future research has to go into the direction of exploring specific inhibitor of S1P Lyase or activators of SphK1 or ways to directly supplement S1P or S1P analogs such as FTY720 *in vivo*.

Succinctly, the present study using rodent and MLE-12 cell culture model concludes that there is a significant increase in the ceramide levels and a significant reduction in the S1P levels that accord with the elevated S1P Lyase expression after high tidal volume mechanical ventilation and high magnitude cyclic stretch in mouse lung and murine alveolar type-II cells respectively. It opens new era of therapeutic potential and we envision a nanocarrier that would site-specifically deliver the S1P Lyase inhibitor or SphK1 activator, that would contribute to the elevation of S1P levels, specifically to the pulmonary epithelium/ endothelium before the commencement of mechanical ventilation.

## CITED LITERATURE:

1. Mammoto, Tadanori, Akiko Mammoto, and Donald E. Ingber. "Mechanobiology and developmental control." *Annual review of cell and developmental biology* 29 (2013): 27-61.
2. Wang, Ning, Jessica D. Tytell, and Donald E. Ingber. "Mechanotransduction at a distance: mechanically coupling the extracellular matrix with the nucleus." *Nature reviews Molecular cell biology* 10, no. 1 (2009): 75-82.
3. Veldhuizen, Ruud, Kaushik Nag, Sandra Orgeig, and Fred Possmayer. "The role of lipids in pulmonary surfactant." *Biochimica et Biophysica Acta (BBA)-Molecular Basis of Disease* 1408, no. 2 (1998): 90-108.
4. Haitzma, Jack J. "Physiology of mechanical ventilation." *Critical care clinics* 23, no. 2 (2007): 117-134.
5. Chatburn, Robert L., Mohamad El Khatib, and Eduardo Mireles-Cabodevila. "A Taxonomy for Mechanical Ventilation: 10 Fundamental Maxims." *Respiratory care* (2014): respcare-03057.
6. Hill, Kylie, and Anne E. Holland. "Strategies to Enhance the Benefits of Exercise Training in the Respiratory Patient." *Clinics in chest medicine* 35, no. 2 (2014): 323-336.
7. Rea-Neto, Alvaro, N. C. Youssef, Fabio Tuche, Frank Brunkhorst, V. Marco Ranieri, Konrad Reinhart, and Yasser Sakr. "Diagnosis of ventilator-associated pneumonia: a systematic review of the literature." *Crit Care* 12, no. 2 (2008): R56.
8. Vitacca, M., Foglio Rubini, K. Foglio, S. Scalvini, S. Nava, and N. Ambrosino. "Non-invasive modalities of positive pressure ventilation improve the outcome of acute exacerbations in COLD patients." *Intensive care medicine* 19, no. 8 (1993): 450-455.
9. Antonelli, Massimo, Giorgio Conti, Luigi Riccioni, and Gianfranco Umberto Meduri. "Noninvasive positive-pressure ventilation via face mask during bronchoscopy with BAL in high-risk hypoxemic patients." *CHEST Journal* 110, no. 3 (1996): 724-728.
10. Bansal, Ruchi, Adebayo Esan, Dean Hess, Luis F. Angel, Stephanie M. Levine, Tony George, and Suhail Raoof. "Mechanical ventilatory support in potential lung donor patients." *CHEST Journal* 146, no. 1 (2014): 220-227.
11. Garg, Shalabh, and Sunil Sinha. "Non-invasive ventilation in premature infants: Based on evidence or habit." *Journal of clinical neonatology* 2, no. 4 (2013): 155.

12. Sutherasan, Yuda, Maria Vargas, and Paolo Pelosi. "Protective mechanical ventilation in the non-injured lung: review and meta-analysis." *Critical Care* 18, no. 2 (2014): 211.
13. Slutsky AS, Ranieri Ventilator-induced lung injury. *VM N Engl J Med.* 2013 Nov 28; 369(22):2126-36.
14. David W. Chang. *Clinical application of mechanical ventilation: workbook.* Clifton Park, NY : Thompson/Delmar Learning, c2006 ISBN: 0766813770 9780766813779
15. DiPaolo, Brian C., and Susan S. Margulies. "Rho kinase signaling pathways during stretch in primary alveolar epithelia." *American Journal of Physiology-Lung Cellular and Molecular Physiology* 302, no. 10 (2012): L992-L1002.
16. Tschumperlin, Daniel J., and Susan S. Margulies. "Equibiaxial deformation-induced injury of alveolar epithelial cells in vitro." *American Journal of Physiology-Lung Cellular and Molecular Physiology* 275, no. 6 (1998): L1173-L1183.
17. Tschumperlin, Daniel J., Jane Oswari, And And Susan S. Margulies. "Deformation-induced injury of alveolar epithelial cells: effect of frequency, duration, and amplitude." *American journal of respiratory and critical care medicine* 162, no. 2 (2000): 357-362.
18. Civelekoglu, G., Y. Tardy, and J-J. Meister. "Modeling actin filament reorganization in endothelial cells subjected to cyclic stretch." *Bulletin of mathematical biology* 60, no. 6 (1998): 1017-1037.
19. Lacolley, Patrick. "Mechanical influence of cyclic stretch on vascular endothelial cells." *Cardiovascular research* 63, no. 4 (2004): 577-579.
20. Morioka, Masataka, Harikrishnan Parameswaran, Keiji Naruse, Masashi Kondo, Masahiro Sokabe, Yoshinori Hasegawa, Béla Suki, and Satoru Ito. "Microtubule dynamics regulate cyclic stretch-induced cell alignment in human airway smooth muscle cells." *PloS one* 6, no. 10 (2011): e26384.
21. Merrill Jr, Alfred H., E. M. Schmelz, D. L. Dillehay, S. Spiegel, J. A. Shayman, J. J. Schroeder, R. T. Riley, K. A. Voss, and E. Wang. "Sphingolipids—the enigmatic lipid class: biochemistry, physiology, and pathophysiology." *Toxicology and applied pharmacology* 142, no. 1 (1997): 208-225.
22. Natarajan, Viswanathan, Steven M. Dudek, Jeffrey R. Jacobson, Liliana Moreno-Vinasco, Long Shuang Huang, Taimur Abassi, Biji Mathew et al. "Sphingosine-1-Phosphate, FTY720, and Sphingosine-1-Phosphate Receptors in the Pathobiology of Acute Lung Injury." *American journal of respiratory cell and molecular biology* 49, no. 1 (2013): 6-17.

23. Maceyka, Michael, Kuzhuvelil B. Harikumar, Sheldon Milstien, and Sarah Spiegel. "Sphingosine-1-phosphate signaling and its role in disease." *Trends in cell biology* 22, no. 1 (2012): 50-60.
24. Morales A, Fernandez-Checa JC. Pharmacological modulation of sphingolipids and role in disease and cancer cell biology. *Mini Rev Med Chem*. 2007 Apr; 7(4):371-82.
25. Don, Anthony S., Carolina Martinez-Lamenca, William R. Webb, Richard L. Proia, Ed Roberts, and Hugh Rosen. "Essential requirement for sphingosine kinase 2 in a sphingolipid apoptosis pathway activated by FTY720 analogues." *Journal of Biological Chemistry* 282, no. 21 (2007): 15833-15842.
26. Berdyshev EV, Gorshkova IA, Garcia JG, Natarajan V, Hubbard WC. Quantitative analysis of sphingoid base-1-phosphates as bisacetylated derivatives by liquid chromatography-tandem mass spectrometry. *Anal Biochem*. 2005 Apr 1;339(1):129-36.
27. K. Hanada, "Serine palmitoyltransferase, a key enzyme of sphingolipid metabolism," *Biochimica et Biophysica Acta*, vol. 1632, no. 1-3, pp. 16-30, 2003.
28. Merrill AH Jr. De novo sphingolipid biosynthesis: a necessary, but dangerous, pathway. *J Biol Chem* 2002; 277:25843-25846.
29. Perrotta C, Clementi E. Biological roles of acid and neutral sphingomyelinases and their regulation by nitric oxide. *Physiology (Bethesda)* 2010; 25:64-71.
30. Maceyka M, Spiegel S. Sphingolipid metabolites in inflammatory disease. *Nature*. 2014 Jun 5; 510(7503):58-67.
31. Spiegel S, Milstien S. Sphingosine-1-phosphate: an enigmatic signalling lipid. *Nat Rev Mol Cell Biol*. 2003 May; 4(5):397-407.
32. Rosen, Hugh, Pedro J. Gonzalez-Cabrera, M. Germana Sanna, and Steven Brown. "Sphingosine 1-phosphate receptor signaling." *Annual review of biochemistry* 78 (2009): 743-768.
33. Fukuhara, Shigetomo, Szandor Simmons, Shunsuke Kawamura, Asuka Inoue, Yasuko Orba, Takeshi Tokudome, Yuji Sunden et al. "The sphingosine-1-phosphate transporter Spns2 expressed on endothelial cells regulates lymphocyte trafficking in mice." *The Journal of clinical investigation* 122, no. 4 (2012): 1416-1426.
34. Tirodkar, T. S., and C. Voelkel-Johnson. "Sphingolipids in apoptosis." *Exp. Oncol* 34, no. 3 (2012): 231-242.
35. Hannun, Yusuf A., and Lina M. Obeid. "Principles of bioactive lipid signalling: lessons from sphingolipids." *Nature reviews Molecular cell biology* 9, no. 2 (2008): 139-150.

36. Wang, Lichun, and Steven M. Dudek. "Regulation of vascular permeability by sphingosine 1-phosphate." *Microvascular research* 77, no. 1 (2009): 39-45.
37. Thammanomai, Apiradee, Hiroshi Hamakawa, Erzsébet Bartolák-Suki, and Béla Suki. "Combined effects of ventilation mode and positive end-expiratory pressure on mechanics, gas exchange and the epithelium in mice with acute lung injury." *PloS one* 8, no. 1 (2013): e53934.
38. Loren A. Mathesona, N. Jack Fairbankb, Geoffrey N. Maksymb, J. Paul Santerrec, Rosalind S. Labowa,d, Characterization of the Flexcell™ Uniflex™ cyclic strain culture system with U937 macrophage-like cells *Biomaterials* 27 (2006) 226–233
39. Qu, M. J., B. Liu, H. Q. Wang, Z. Q. Yan, B. R. Shen, and Z. L. Jiang. 2007. Frequency-dependent phenotype modulation of vascular smooth muscle cells under cyclic mechanical strain. *J. Vasc. Res.* 44:345–353.
40. Bo Liu, Ming-Juan Qu, [...], and Zong-Lai Jiang Role of Cyclic Strain Frequency in Regulating the Alignment of Vascular Smooth Muscle Cells In Vitro *Nov 2007 Biophys J.* Feb 15, 2008; 94(4): 1497–1507.
41. Birukov, Konstantin G., Jeffrey R. Jacobson, Alejandro A. Flores, Q. Ye Shui, Anna A. Birukova, Alexander D. Verin, and Joe GN Garcia. "Magnitude-dependent regulation of pulmonary endothelial cell barrier function by cyclic stretch." *American Journal of Physiology-Lung Cellular and Molecular Physiology* 285, no. 4 (2003): L785-L797.
42. Vogel, Peter, Michael S. Donoviel, Robert Read, Gwenn M. Hansen, Jill Hazlewood, Stephen J. Anderson, Weimei Sun, Jonathan Swaffield, and Tamas Oravec. "Incomplete inhibition of sphingosine 1-phosphate lyase modulates immune system function yet prevents early lethality and non-lymphoid lesions." *PloS one* 4, no. 1 (2009): e4112.
43. Zhao, Yutong, Irina A. Gorshkova, Evgeny Berdyshev, Donghong He, Panfeng Fu, Wenli Ma, Yanlin Su et al. "Protection of LPS-induced murine acute lung injury by sphingosine-1-phosphate lyase suppression." *American journal of respiratory cell and molecular biology* 45, no. 2 (2011): 426-435.
44. Nicholson, Donald W., Ambereen Ali, Nancy A. Thornberry, John P. Vaillancourt, Connie K. Ding, Michel Gallant, Yves Gareau et al. "Identification and inhibition of the ICE/CED-3 protease necessary for mammalian apoptosis." (1995): 37-43.
45. Fernandes-Alnemri, Teresa, Gerald Litwack, and Emad S. Alnemri. "CPP32, a novel human apoptotic protein with homology to *Caenorhabditis elegans* cell death protein Ced-3 and mammalian interleukin-1 beta-converting enzyme." *Journal of Biological Chemistry* 269, no. 49 (1994): 30761-30764.

46. Lazebnik, Y. A., S. H. Kaufmann, S. Desnoyers, G. G. Poirier, and W. C. Earnshaw. "Cleavage of poly (ADP-ribose) polymerase by a proteinase with properties like ICE." (1994): 346-347.
47. Rieger, Aja M., Kimberly L. Nelson, Jeffrey D. Konowalchuk, and Daniel R. Barreda. "Modified annexin V/propidium iodide apoptosis assay for accurate assessment of cell death." *Journal of visualized experiments: JoVE* 50 (2011).
48. Schwab SR, Pereira JP, Matloubian M, Xu Y, Huang Y, Cyster JG (2005) Lymphocyte sequestration through S1P lyase inhibition and disruption of S1P gradients. *Science* 309:1735–1739
49. <http://www.flexcellint.com/applications1.html>  
  
<http://www.flexcellint.com/documents/FlexJrTensionManual>  
Viewed on 10/14/2014
50. Xu Dong, L. I. A. O., W. A. N. G. Xiao Hui, J. I. N. Hai Jing, C. H. E. N. Lan Ying, and C. H. E. N. Quan. "Mechanical stretch induces mitochondria-dependent apoptosis in neonatal rat cardiomyocytes and G2/M accumulation in cardiac fibroblasts." *Cell research* 14, no. 1 (2004): 16-26.
51. Kenneth E. Chapman, Scott E. Sinclair, Daming Zhuang, Aviv Hassid, Leena P. Desai, and Christopher M. Waters Cyclic mechanical strain increases reactive oxygen species production in pulmonary epithelial cells. *Am J Physiol Lung Cell Mol Physiol* 289: L834–L841, 2005.
52. Halbertsma, F. J., M. Vaneker, G. J. Scheffer, and J. G. Van Der Hoeven. "Cytokines and bio-trauma in ventilator-induced lung injury: a critical review of the literature." *Neth J Med* 63, no. 10 (2005): 382-392.
53. Kobayashi, Tsutomu, Keiko Nitta, Masaya Ganzuka, Sachiko Inui, Gertie Grossmann, and Bengt Robertson. "Inactivation of exogenous surfactant by pulmonary edema fluid." *Pediatric research* 29, no. 4 (1991): 353-356.
54. Lim, Lina HK, and Elizabeth M. Wagner. "Airway distension promotes leukocyte recruitment in rat tracheal circulation." *American journal of respiratory and critical care medicine* 168, no. 9 (2003): 1068-1074.
55. zu Heringdorf, Dagmar Meyer, Katja Ihlefeld, and Josef Pfeilschifter. "Pharmacology of the sphingosine-1-phosphate signalling system." In *Sphingolipids: Basic Science and Drug Development*, pp. 239-253. Springer Vienna, 2013.

APPENDIX



Office of Animal Care and  
 Institutional Biosafety Committees (MC 672)  
 Office of the Vice Chancellor for Research  
 206 Administrative Office Building  
 1737 West Polk Street  
 Chicago, Illinois 60612-7227

March 5, 2013

Viswanathan Natarajan  
 Pharmacology  
 M/C 868

Dear Dr. Natarajan:

The protocol indicated below was reviewed at a convened ACC meeting in accordance with the Animal Care Policies of the University of Illinois at Chicago on 1/15/2013. *The protocol was not initiated until final clarifications were reviewed and approved on 2/21/2013. The protocol is approved for a period of 3 years with annual continuation.*

**Title of Application:** Mechanisms of Acute Lung Injury

**ACC Number:** 12-246

**Initial Approval Period:** 2/21/2013 to 1/15/2014

**Current Funding:** *Portions of this protocol are supported by the funding sources indicated in the table below.*

**Number of funding sources:** 2

Funding Agency	Funding Title			Portion of Proposal Matched
NIH	<i>Cytoskeletal regulation of lung endothelial pathobiology (For project 3)</i>			<i>Protocol is linked to form G</i> <i>ACC 10-078</i>
Funding Number	Current Status	UIC PAF NO.	Performance Site	Funding PI
<i>P01 HL058064</i>	<i>Funded</i>	<i>201203532</i>	<i>UIC</i>	<i>Joe GN Garcia</i>
Funding Agency	Funding Title			Portion of Proposal Matched
NIH	<i>Role of sphingolipids in the pathobiology of lung injury (Project 1)</i>			<i>Protocol is linked to form G</i> <i>ACC 11-004</i>
Funding Number	Current Status	UIC PAF NO.	Performance Site	Funding PI
<i>P01 HL098050</i>	<i>Funded</i>	<i>201007207</i>	<i>UIC</i>	<i>Viswanathan Natarajan</i>

This institution has Animal Welfare Assurance Number A3460.01 on file with the Office of Laboratory Animal Welfare (OLAW), NIH. This letter may only be provided as proof of IACUC approval for those specific funding sources listed above in which all portions of the funding proposal are matched to this ACC protocol.

In addition, all investigators are responsible for ensuring compliance with all federal and institutional policies and regulations related to use of animals under this protocol and the funding sources listed on this protocol. Please use OLAW's "*What Investigators Need to Know about the Use of Animals*" (<http://grants.nih.gov/grants/olaw/InvestigatorsNeed2Know.pdf>) as a reference guide. Thank you for complying with the Animal Care Policies and Procedures of UIC.

Sincerely yours,



Bradley Merrill, PhD  
Chair, Animal Care Committee

BM/mbb

cc: BRL, ACC File, Panfeng Fu

Office of Animal Care and Institutional  
Biosafety Committee (OACIB) (M/C 672)  
Office of the Vice Chancellor for Research  
206 Administrative Office Building  
1737 West Polk Street  
Chicago, Illinois 60612

1/15/2014

Viswanathan Natarajan  
Pharmacology  
M/C 868

Dear Dr. Natarajan:

The protocol indicated below was reviewed in accordance with the Animal Care Policies and Procedures of the University of Illinois at Chicago and renewed on 1/15/2014.

**Title of Application:** Mechanisms of Acute Lung Injury  
**ACC NO:** 12-246  
**Original Protocol Approval:** 2/21/2013 (3 year approval with annual continuation required).  
**Current Approval Period:** 1/15/2014 to 1/15/2015

**Funding:** Portions of this protocol are supported by the funding sources indicated in the table below.  
**Number of funding sources:** 2

Funding Agency	Funding Title			Portion of Funding Matched
NIH	Cytoskeletal regulation of lung endothelial pathobiology (For project 3)			Protocol is linked to form G ACC 10-078
Funding Number	Current Status	UIC PAF NO.	Performance Site	Funding PI
P01 HL038064	Funded	2012-03532	UIC	Joe GN Garcia
Funding Agency	Funding Title			Portion of Funding Matched
NIH	Role of sphingolipids in the pathobiology of lung injury (Project 1)			Protocol is linked to form G ACC 11-004
Funding Number	Current Status	UIC PAF NO.	Performance Site	Funding PI
P01 HL098050	Funded	2010-07207	UIC	Viswanathan Natarajan

This institution has Animal Welfare Assurance Number A3460.01 on file with the Office of Laboratory Animal Welfare, NIH. This letter may only be provided as proof of IACUC approval for those specific funding sources listed above in which all portions of the grant are matched to this ACC protocol.

Thank you for complying with the Animal Care Policies and Procedures of the UIC.

Sincerely,



Bradley Merrill, PhD  
Chair, Animal Care Committee

BM/kg  
cc: BRL, ACC File, Panfeng Fu

## VITA

### Vidyani Suryadevara

#### **Education**

##### ***Master of Science: Bioengineering***

University of Illinois, Chicago (UIC). (December 2014)

##### ***Bachelor of Technology: Biotechnology***

Chaitanya Bharathi Institute of Technology, Hyderabad, India. (May 2013)

#### **Experience**

- Graduate Teaching Assistant, Biological Sciences Dept., UIC (1/1/2014 – present).  
Microbiology lab (BioS 351)                      Spring 2014  
Microbiology Theory (BioS 350)                Fall 2014

#### **Awards**

- Best oral presentation in International Conference on Nanoscience & Engineering Applications, held at JNTUH, India from 26<sup>th</sup> – 28<sup>th</sup> June, 2014.
- Chancellor's Award for Student Service & Leadership 2014, University of Illinois, Chicago.

#### **Research Papers (Accepted):**

Testai, Fernando; Xu, Hao-Liang; Kilkus, John; Suryadevara, Vidyani; Gorshkova, Irina; Berdyshev, Evgeny; Pelligrino, Dale; Dawson, Glyn Changes in the Metabolism of Sphingolipids after Subarachnoid Hemorrhage Journal of Neuroscience Research

Vidyani Suryadevara<sup>1\*</sup>, Vijayalaxmi Govindugari Exosomes and microparticles: The nanosized vesicles released from the cells that act as biomarkers for disease and treatment – riveting on lung diseases.

#### **Professional activities**

- Treasurer, Graduate Student Council, UIC.
- Secretary and Charter Member, UIC COE Toastmasters Club.
- Member, search advisory committee for the Vice Chancellor for Health Affairs.

Represented UIC at the President's Interfaith and Community Service, held at Washington D.C. from 22-23<sup>rd</sup> September, 2014